# Effect of Localized Muscle Fatigue on Postural Control Stability and Muscle Activation Strategies

**BRANDON HERRON**

Thesis submitted to the University of Ottawa
in partial fulfillment of the requirements for the

**MASTER OF SCIENCE IN HUMAN KINETICS**

School of Human Kinetics
Faculty of Health Sciences
University of Ottawa

## Abstract

Optimal postural control involves the integration of sensory inputs from the visual, vestibular, and proprioceptive systems. It requires both individual muscle activation and intermuscular interactions that adapt balance strategies to task demands, while being shaped by sensory feedback. Neuromuscular fatigue (NMF) is thought to destabilize postural control by degrading proprioceptive reliability and altering muscle activation strategies. Yet, whether fatigue effects generalize across postural contexts remains uncertain. This thesis aimed to examine how NMF influences postural control stability and muscle activation strategies during two tasks of varying stability demands: quiet standing and forward lean. Specifically, we sought to determine how fatigue influences: 1) lower-limb muscle activation, co-contraction patterns and intermuscular coherence, 2) center of pressure (COP) behavior across different time scales, and 3) the relationship between EMG coherence and open- and closed-loop postural control mechanisms inferred from COP Discrete Wavelet Transform analysis. Fourteen healthy adults performed quiet standing and forward-lean tasks with eyes open or closed, before and after a standardized isometric plantarflexion/dorsiflexion fatigue protocol. We quantified neuromuscular activity and coordination (EMG amplitude, co-contraction, intermuscular coherence) as well as postural sway (center-of-pressure (COP) metrics and timescale-specific control (wavelet-based energy). The effects of fatigue and postural task were evaluated using repeated-measures ANOVA models. Pearson's correlations were also used to assess the relationship between changes in EMG and COP variables. Results showed that muscle activation patterns were primarily driven by postural task demands rather than fatigue. Intermuscular coherence analysis revealed task- and frequency-dependent fatigue effects, with agonist-agonist coherence increasing significantly in mid- and high-frequency bands during the most challenging condition (forward lean, eyes-closed) after fatigue ($p < 0.01$). Traditional center of pressure measures showed limited fatigue effects, and discrete wavelet analysis revealed no significant fatigue-induced changes in frequency band energy distributions. These findings demonstrate that NMF produces subtle, task-dependent alterations in postural control that are most evident during challenging postural demands.

**Acknowledgements**

I would like to sincerely acknowledge the support and guidance of my supervisor, Dr. Martin Bilodeau. Martin, thank you so much for this opportunity. You've allowed me to continue my journey as a researcher, and I have nothing but the deepest respect for you. Your invaluable expertise, mentorship, and encouragement have been instrumental throughout the development of this project. The continuous engagement, availability and thoughtful feedback have greatly contributed to my academic growth and to the successful completion of this thesis.

I also extend my gratitude to the members of my thesis committee, Dr. Heidi Sveistrup and Dr. Yves Lajoie, for their constructive input and insightful questions. Their perspectives, especially during the proposal challenged me to think more critically and deeply about my research, strengthening the quality of this work. I further acknowledge the University of Ottawa for providing the academic environment and resources necessary to carry out this project.

On a personal note, I would like to thank the two most important women in my life: my mother and my partner. To my mom, your love, strength, and constant support have carried me through so many challenges. We have been through so much together. I am forever grateful, and I love you deeply. To my partner Yane, we only started out our journey, but I feel like we've done so much already. Thank you for being a constant source of inspiration and patience. Your understanding, especially during the many weekends I spent working on this thesis instead of with you, means more to me than I can put into words. Thank you, my love, for everything.

## Table of Contents

## List of Figures

## List of Tables

## List of Abbreviations and Symbols

| | |
|---|---|
| **AG** | Agonist |
| **ANOVA** | Analysis of Variance |
| **ANT** | Antagonist |
| **AP** | Anteroposterior |
| **APA** | Anticipatory Postural Adjustment |
| **BOS** | Base of Support |
| **CCI** | Co-Contraction Index |
| **COM** | Control Center of Mass |
| **COP** | Center of Pressure |
| **CNS** | Central Nervous System |
| **DF** | Dorsiflexion |
| **DWT** | Discrete Wavelet Transform |
| **EC** | Eyes Closed |
| **EO** | Eyes Open |
| **EMG** | Electromyographic |
| **EMM** | Estimated Margin Mean |
| **FL** | Forward Leaning |
| **GES** | Generalized eta Squared |
| **GG** | Greenhouse–Geisser |
| **GL** | Gastrocnemius Lateralis |
| **GM** | Gastrocnemius Medialis |
| **ML** | Mediolateral |
| **MSC** | Magnitude-Squared Coherence |
| **MVC** | Maximum Voluntary Contraction |
| **MVIC** | Maximum Voluntary Isometric Contraction |
| **NMF** | Neuromuscular Fatigue |
| **PF** | Plantarflexion |
| **QS** | Quiet Standing |
| **RI** | Reciprocal Inhibition |

| | |
|---|---|
| **RMS** | Root Mean Square |
| **RPA** | Reactive Postural Adjustments |
| **SD** | Standard Deviation |
| **SDA** | Stabilogram Diffusion Analysis |
| **SOL** | Soleus |
| **TA** | Tibialis Anterior |
| **WC** | Wavelet Coefficient |

## Chapter 1: Introduction

Postural control is defined as the ability to align and control the body's position in space to achieve stability and orientation. Stability of posture refers to the ability to control center of mass (COM) with respect to the base of support (BOS)[1]. The COM is an imaginary point at which the total body mass can be assumed to be concentrated[2]. The BOS refers to the contact area where the body interfaces with the ground. Along with COM, another commonly used metric to assess postural stability is center of pressure (COP). The center of pressure (COP) represents the resultant of the ground reaction forces; in other words, it is the point location of the total forces acting on the support surface[3]. In the context of postural control, the COP oscillates and continuously adjusts around the COM to maintain equilibrium and stability within the BOS.[3]

In contrast with quiet standing (QS), in forward leaning (FL), the COM is intentionally shifted toward the anterior edge of the base of support, reducing the stability margin and increasing the demands required to regulate the COP. This anterior displacement heightens gravitational torque demands, leading to larger COP excursions and velocity[4]. As a result, FL is commonly used in postural control research to challenge stability[3,5]. The present thesis will contrast the effect of fatigue between QS and FL to assess to what extent the effects of fatigue are dependent on postural task demands.

As the body sways while maintaining an upright standing posture, the ankle plantarflexor and dorsiflexor muscles, in particular, are activated to maintain stability. The soleus (SOL) and gastrocnemius act as a synergistic muscle pair and are the main plantar flexors. On the other hand, the tibialis anterior (TA) acts as the antagonist muscle to the synergistic SO-gastrocnemius pair , but is minimally active under a typical QS[6]. However, as postural challenge increases, the demand for TA activity changes, which may lead to increases or decreases in activation based on the needs of the postural control system under different postural conditions. This thesis will focus on the activation of these two muscle groups under both QS and FL tasks.

Remaining in a stable, upright position while standing also requires the integration of multiple sensory systems (visual, proprioceptive, vestibular) and appropriate coordinated muscle contractions. The combined and partially redundant nature of these sensory systems enhances the

robustness of the postural control system, allowing the neural operator to compensate for sensory perturbations and maintain equilibrium[7]. To effectively incorporate sensory information into an appropriate motor output, the central nervous system employs specific motor control mechanisms. Motor control mechanisms in the control of standing posture involves feedforward (anticipatory) and feedback (reactive) mechanisms. These operate across spinal and supraspinal levels to dynamically adjust postural tone and joint stiffness[8]. These mechanisms are translated into intermuscular coordination patterns, such as altering the activation pattern of synergist muscles or of antagonist muscles through increased co-contraction or reciprocal inhibition in response to task demands, such as forward leaning, or internal perturbations, such as fatigue[8,9].

Coherence analysis is a frequency-domain analysis method that assesses the linear correlation between two distinct signals as a function of frequency[10]. In the context of electrophysiological and biomechanical studies, coherence elucidates the harmonized oscillatory effects that regulate pairs of signals, as evidenced by electromyographic (EMG) activity across various muscles or the interaction between neural and muscular systems[11]. The computation of coherence involves the normalized cross-spectrum of two signals, producing numerical outputs that fluctuate between 0 (representing a total lack of mutual engagement) and 1 (indicating a perfect linear relationship)[12]. In this thesis, we will use coherence analysis to assess common inputs to both agonist and antagonist muscle pairs, thereby providing more detailed information concerning how muscle activation can change following a fatiguing exercise.

As a complement to EMG coherence, we will also employ the Discrete Wavelet Transform (DWT) in this thesis. The DWT is a method for time-frequency decomposition of signals at various resolutions. Unlike Fourier techniques that presume stationarity, wavelet analysis is adept at handling non-stationary physiological data. The DWT decomposes signals into approximation and detail coefficients, isolating energy contributions across frequency bands while maintaining temporal localization. This characteristic makes it particularly effective for the analysis of center-of-pressure (COP) trajectories[13,14]. In particular, we will use such an analysis technique to elucidate the role of feedforward and feedback control mechanisms in QS and FL tasks, and how fatigue affects those.

Neuromuscular fatigue (NMF) can alter the capacity of muscles to generate corrective forces and alter proprioception, and this has direct implications for postural control. During quiet standing,

fatigue of the ankle musculature can reduce the efficiency of fine torque adjustments, leading to greater COP variability and increased reliance on sensory feedback for stability[15,16]. In forward leaning, where the COM is positioned closer to the anterior stability boundary, fatigue effects could be magnified.[17–19] Notably, the application of DWT to examine frequency-specific fatigue effects on COP dynamics, particularly when integrated with intermuscular coherence analysis, represents a relatively novel methodological approach that can provide new insights into the neural and biomechanical adaptations underlying postural control under fatigue[20]. This thesis project will use both coherence analysis of agonists and antagonists EMG signals and DWT of COP displacements to characterize the effect of neuromuscular fatigue on postural control mechanisms during two tasks of varying difficulty, quiet standing and a forward leaning task.

## 1.1. Research Aims

- **Research Questions**

**1)** How does neuromuscular fatigue change muscle activation strategies of the lower leg, as determined through EMG coherence, during quiet standing and a forward-leaning task under eyes open and eyes closed conditions?

**2)** How do the effects of neuromuscular fatigue of the leg on postural control measured by center of pressure displacement behaviours in long-term and short-term timescales, differ between quiet stance and a forward-leaning task?

**3)** How do the characteristics of COP displacement, distinguished as open-loop and closed-loop behaviours associate with EMG coherence under neuromuscular fatigue during quiet standing and a forward-leaning task?

- **Objectives**

**1)** To compare the effects of fatigue on lower limb muscle activation patterns, including co-activation and coherence, between quiet standing and forward leaning tasks under eyes-open and eyes-closed conditions.

**2)** To compare the effects of fatigue on traditional and long-term and short-term COP characteristics under increasingly difficult postural demands (e.g., between quiet standing and forward leaning tasks under eyes-closed and eyes-open).

**3)** To assess the association/correlation between fatigue-related changes in muscle activation and COP characteristics in both quiet standing and forward leaning tasks.

- **Hypotheses**

**1)** Following neuromuscular fatigue, postural control strategies and muscle activity are expected to change by:

- **a.** Increase in EMG signal amplitudes across all monitored muscle groups.
- **b.** A compensatory co-contraction strategy during both quiet standing and forward-leaning postural tasks, with greater co-activation patterns observed during increasingly difficult postural demands (e.g., eyes-closed during a forward-leaning task).
- **c.** Enhanced intermuscular coherence among agonist muscle pairs across both tasks, accompanied by increased coherence between antagonist muscles in both postural task with more pronounced antagonist muscle coherence during the forward leaning task under eyes-closed condition.

**2)** Neuromuscular fatigue is expected to result in increased postural instability, as evidenced by:

- **a.** Center of pressure (COP) amplitude and velocity increase during both postural tasks, with greater increases observed under higher postural demands, which is during the forward-leaning task and eyes-closed condition.
- **b.** Greater contribution of closed-loop long-term behaviour, with a more pronounced effect observed with increasingly difficult postural demands (e.g., during the forward-leaning, eyes-closed task).

**3)** A significant association between fatigue-related changes in low-frequency plantar flexors coherence and closed loop behaviour of center of pressure signals. This linkage is expected because low-frequency coherence (<1 Hz) and closed-loop COP behavior operate on matched timescales (>1 second), with both reflecting slow, feedback-dependent sensory-motor integration processes that generate sustained corrective responses to maintain postural stability[21,22].

# Chapter 2: Literature Review

This review of the literature explores how the postural control system integrates multisensory information with neuromuscular strategies to maintain stability across tasks of varying difficulty. It begins by outlining the interplay between voluntary and automatic mechanisms, emphasizing how passive and active contributors to muscle and joint stiffness, particularly co-contraction (which increases joint stiffness) and the modulation of reciprocal inhibition (which normally suppresses antagonist activity), support joint stabilization and movement efficiency. The co-contraction Index (CCI) is introduced as a practical proxy for documenting active stiffness. Neural coordination is then considered through frequency-specific intermuscular coherence, where band-limited analyses provide indirect evidence about the relative involvement of subcortical versus corticospinal control. Next, the review characterizes feedforward (open-loop) and feedback (closed-loop) processes, highlighting how visual, vestibular, and somatosensory cues are integrated and dynamically reweighted as environmental reliability and task demands change; where relevant, discrete wavelet decomposition is used to resolve time–frequency structure underlying these adjustments. Finally, the review examines how neuromuscular fatigue perturbs sensory processing, muscle activation strategies, intermuscular coherence, and postural outcomes, drawing together convergent and divergent findings across paradigms.

## 2.1. Integrating Sensory Input and Muscle Activation in Postural Control Strategies

Postural control is a complex motor skill that relies on multiple mechanisms to maintain postural stability. Effective postural regulation requires not only the activation of individual muscles to stabilize the body, but also the integration of intermuscular interactions that support adaptive balance strategies under varying task demands, and shaped by sensory feedback (e.g., visual, proprioceptive, and vestibular) and other factors (e.g., neuromuscular fatigue). Such balance strategies can involve corticospinal, subcortical, and spinally mediated mechanisms (some are discussed in more detail in the next section), and it has also been suggested that these can be inferred from the breakdown of electromyographic (EMG) signals into different frequency ranges[23,24] (see 2.2.2 below).

## 2.2. Neuromuscular Mechanisms Underlying Postural Control

Muscle stiffness results from the combined contribution of passive and active mechanisms and is essential for maintaining postural stability. Passive muscle stiffness refers to the resistance provided by non-contractile tissues such as the elastic structures (e.g., tendons, ligaments, and joint capsules). This baseline stiffness exists without muscle activation. However, passive stiffness alone is relatively low at the normal standing posture and is generally insufficient to stabilize the upright body by itself during high postural demands[25]. By contrast, active muscle stiffness is generated by muscle contractions. In the context of postural control, when the muscles spanning the ankle (dorsiflexors in the front of the leg and plantarflexors in the calf) are actively engaged, together with the knee extensors and flexors, hip extensors, flexors, abductors and adductors, and trunk stabilizers (paraspinals and abdominal wall), their tensile forces create restoring torques across joints and coordinate ankle–hip–trunk synergies to maintain the COM over the BOS[3,26]. This active component includes short-latency, spinally mediated feedback responses, which resist length changes when the muscle is activated in response to a stimulus, such as a stretch[27]. Active stiffness also arises from voluntary activation and co-contraction of agonist and antagonist muscles, allowing the nervous system to tune joint impedance in anticipation of or during postural and motor tasks[28]. In essence, active stiffness arises from the neural activation of muscles, which can stiffen the joint far beyond the passive baseline by increasing (co)activation of the agonist and antagonist muscles around the ankle. In contrast, reciprocal inhibition (RI) facilitates joint mobility and efficient force production by reducing the activity of the antagonist muscle during agonist contraction. This neural mechanism allows for smoother and more coordinated movements by minimizing unnecessary resistance, and it plays a particularly important role during dynamic balance tasks where rapid adjustments are required[29]. Together, RI and co-contraction illustrate two contrasting muscle activation strategies, representing only a subset of the mechanisms through which the neuromuscular system adapts to varying postural demands.

### 2.2.1. Postural Control and Active Stiffness Regulation

A common proxy into active stiffness involves quantifying the co-contraction of muscle groups through the Co-Contraction Index (CCI), a quantitative measure of the level of simultaneous activation in antagonist muscle pairs. The CCI concept was introduced by Falconer and Winter

(1985) as a way to quantify the overlapping activity of antagonistic muscles from their EMG signals[30]. In the context of postural control at the ankle joint, a high CCI value would be indicative of both dorsiflexors and plantarflexors being active together to a large degree, whereas a low CCI means little overlap. When postural stability is challenged, the amount of antagonistic co-activation (as captured by CCI) increases and largely governs the stiffness across the joint that resists swaying[31].

Examples of these patterns have been documented in prior work. For instance, Kim and Hwang showed that when subjects responded to small perturbations in the anterior-posterior plane, they relied on a strategy of increasing ankle stiffness, evidenced by a rise in CCI rather than generating large ankle movements[31]. Likewise, comparisons of young vs. elderly adults have noted that elderly individuals often exhibit a greater CCI during quiet stance, indicating a preference for a stiffening strategy, though the co-contraction strategy has been associated with increased postural sway (discussed later)[6].

In response to postural perturbations, individuals often increase active joint stiffness by recruiting antagonist muscle groups, a strategy thought to enhance muscle stability and improve postural control under challenging conditions[3,6,31]. While some studies support joint stiffness as a stabilizing strategy[3], other empirical findings have questioned its role, suggesting that increased co-contraction does not always translate into improved postural stability under heightened task demands. Notably, negative associations between co-contraction and stability have been observed during unpredicted pertubations[32] and during static bipedal stance[6,33].

Donath and collaborators found amplified co-activation of the tibialis anterior and gastrocnemius medialis during more challenging postural tasks, such as single-leg stance with eyes closed compared to bipedal quiet standing with eyes open[34]. Warnica et al. reported that increased co-contraction was associated with higher center of mass (COM) and center of pressure (COP) velocities[33] . These elevated COM and COP velocities can be indicative of greater postural instability and greater fall risk[35]. Additionally, increased active co-contraction of TA during a typical quiet stance results in increased COP velocity, though this effect was seen in seniors only[36]. Furthermore, seniors under similar task demands as their young counter-parts present with increased co-contraction of the tibialis anterior and increased postural sway seen through increase path length of COP[34]. Contrary to these findings, Carpenter et al. quantified ankle stiffness and

found a negative association between ankle stiffness and COP displacement[37]. While evidence appears consistent when considering velocity and co-contraction metrics, alternative COP measures present a less conclusive picture.

In contrast, reciprocal inhibition (RI) is a spinal reflex that supports postural control by coordinating opposing muscle groups: activation of an agonist sends Ia-afferent input to inhibitory interneurons, which suppress antagonist α-motoneurons and limit unnecessary co-contraction, enabling efficient sway corrections and weight shifts. This mechanism is well established in animal and human preparations, and is modulated by task demands during balance behaviors[29,38].

When reciprocal inhibition is compromised, the consequences for postural control can be significant. Dysfunctions such as Parkinson's disease, post-stroke hemiparesis, and cerebellar ataxia, can lead to excessive antagonist muscle co-activation, resulting in joint stiffness, delayed responses, and inability to make the fine-tuned adjustments required to recover from balance perturbations[39–42]. This impairment is directly linked to increased fall risk, as individuals cannot effectively respond to losses of balance in time[40,43]. The resulting muscle co-contraction and rigidity remove a critical stabilizing element of motor control, making reciprocal inhibition dysfunction a key factor in understanding balance disorders and fall prevention. Despite CCI use in the literature, only a limited subset of studies has jointly manipulated fatigue with postural task and/or vision; these investigations are typically narrow in scope (single-task paradigms, small samples) and yield mixed, non-generalizable effects. Consequently, the behavior of the CCI in fatigue-related postural control remains incompletely characterized across tasks and sensory contexts.

### 2.2.2. Frequency-Specific Coherence as a Measure of Muscle Synchronization in Postural Control

Synchronization between synergistic and antagonistic muscles can be assessed using time-domain cross-correlation or frequency-domain coherence analysis. A key advantage of coherence analysis is its ability to quantify the correlation in the activation of muscle groups across the full frequency spectrum[24]. In other words, coherence provides additional information that extends beyond the overall synchronization of muscle activity, providing depth of analysis into corticospinal and

subcortical processes from different frequency components[23,44,45]. In this method, the cross-spectral density of the paired EMG signals is computed from their individual power spectra. The squared magnitude of the cross-spectrum is then normalized by the product of the autospectral densities of each signal to yield the magnitude-squared coherence (MSC) function (Eq. 9). MSC values may subsequently be examined within discrete frequency bands to characterize the frequency-specific strength of muscle synchronization[23].

In this thesis, we adopt the band nomenclature proposed by Nandi and colleagues to base our physiological interpretation of frequency-specific EMG coherence features[45]. For instance, high-frequency band activity (15–35 Hz) is linked to motor preparation and is thought to correlate with corticospinal processes[12,46]. High-band intermuscular coherence is retained in progressive muscular atrophy but markedly reduced in primary lateral sclerosis, indicating dependence on an intact corticospinal tract[47]. After complete spinal cord injury, coupling shifts to low frequencies around 2–13 Hz and beta-band coherence is absent, consistent with loss of supraspinal drive[48]. In contrast, it has been suggested that low-band activity (0–5 Hz) is generally associated largely with subcortical processes[44,45,49], though the evidence remains less conclusive than that for higher band contributions. In the context of postural control, neural activity within the low-frequency band may reflect automatic processes engaged in stabilizing posture, whereas high-band activity is more likely to represent voluntary control reflective of cortical input mechanisms within the postural control system[23,45].

Coherence is widely used to infer shared neural drive during stance, yet its application to fatigue-related postural control is limited. Most studies either examine quiet stance without fatigue, task difficulty, or vision[50,51], or they report fatigue-related coherence changes outside postural tasks (e.g., hand muscles) without linking changes to COP outcomes or joint-stiffness measures[52]. Together, this leaves unclear when and how fatigue alters frequency-specific coupling of agonist–antagonist ankle muscles under fatigue in ways that translate to postural control mechanisms. In the present thesis, this method of analysis is used to provide more detailed information in how the postural control system is regulated under a fatigued state.

## 2.3. Sensory Input and Control Mechanisms

To initiate muscle activation strategies, the body relies on both feedforward (proactive) processes and feedback (reactive) processes, which can be understood through the concepts of open-loop and closed-loop control. Feedforward postural control refers to anticipatory adjustments made by the nervous system in advance of a predicted disturbance or voluntary movement. Anticipatory postural adjustments (APAs) involve activating postural muscles in a feedforward manner; for example, before a voluntary movement begins, in anticipation of the destabilizing forces that the movement will cause [53]. Feedback postural control, on the other hand, is the reactive adjustments that occur in response to sensory feedback indicating a postural disturbance or error. These responses are often called compensatory or reactive postural adjustments (RPAs) and are typically evoked by unexpected external perturbations or by errors in executing movements[54].

### 2.3.1. Feedback and Feedforward Processing

In postural control, open-loop processes are mechanisms that do not depend on immediate feedback as they are initiated through pre-planned actions. Closed-loop processes, on the other hand, continually use sensory feedback to compare the actual posture against a desired state and adjust muscle outputs to reduce any error. In essence, feedforward postural adjustments are implemented in an open-loop manner responding to pre-emptive signals, whereas feedback adjustments are part of a closed-loop control modulated by ongoing sensory signals. Human postural control during an upright stance is maintained through both modes: there are short-term intervals where posture behaves as if under open-loop control, and longer-term regulation that clearly involves closed-loop feedback[21]. The combined efforts of open-loop and closed-loop control function to maintain balance in the presence of internal and external perturbances that threaten balance, such as unstable postures and fatigue[55].

Open-loop postural control refers to pre-set or feedforward commands that are not continuously adjusted by sensory feedback during execution. One component is musculoskeletal mechanics, such as the passive stiffness. This passive stability acts in open-loop fashion as it does not change based on sensory input, but it provides a baseline resistance to sway[56]. Another open-loop element is the anticipatory feedforward actions described earlier (APAs), which are executed without waiting for error signals[56]. Open-loop control is advantageous given the delays in biological

feedback loops; by the time the nervous system processes a tilt via sensory feedback, the body could already be well into a fall; therefore, having some built-in, feedforward stabilization and passive stability provides additional time.

Closed-loop postural control is engaged when the system uses sensory feedback to generate corrective actions. In standing balance, once the body's sway reaches threshold points which jeopardize postural stability, the nervous system actively intervenes operating in closed-loop fashion to drive the center of mass to more stable positions. In a closed-loop system, any deviation from upright stance produces an error signal (via sensory receptors) and the CNS attempts to minimize that error by adjusting muscle forces. Examples of these mechanisms are seen through the generation of active stiffness via co-contraction or reciprocal inhibition during increasingly difficult tasks, which may operate under both open-loop (anticipatory) and closed-loop (feedback) control processes, depending on whether the response precedes or follows a perturbation[8,57,58].

### 2.4. Sensory System Inputs and Postural Control

The feedback mechanisms of postural control during an upright stance require the integration of sensory information from the visual, vestibular, and somatosensory systems, to optimally maintain postural stability [59–61]. Visual signals provide information about the external environment and motion of the visual field, vestibular organs in the inner ear sense head orientation and acceleration relative to gravity, and somatosensory receptors (proprioceptive and cutaneous inputs) inform about body segment positions and contact with the support surface[62]. The CNS continuously integrates these afferent inputs to construct an internal model of body position and movement. This multisensory assimilation enables the CNS to actively modulate muscle activation patterns and coordinate motor responses that counteract destabilizing forces[59].

#### 2.4.1. The Visual Sensory System and Postural Control

Visual sensors play a critical role in detecting head position relative to objects within the visual field, thereby constructing a spatial map that guides navigation through the environment[61]. Visual cues provide essential information regarding the perception of potential hazards, surrounding movements, and the individual's own body motion in relation to the environment[63]. Therefore,

vision has significant implications for maintaining postural stability across a wide range of postural tasks in all individuals[63].

### 2.4.2. The Vestibular Sensory System and Postural Control

The vestibular system plays a crucial role in detecting head position and motion relative to gravity, while also contributing to visual stabilization during head movements through the vestibulo-ocular reflex[63,64]. Vestibular signals, relayed to the spinal cord and brainstem, also drive reflexes that coordinate head, neck, and trunk movements to support postural alignment[65]. However, in healthy adults standing on a stable surface, somatosensory information is generally more dominant for postural control[66]. This has been seen when proprioceptive or visual inputs are reduced, the CNS increases reliance on vestibular cues to maintain balance[61,67]. These findings demonstrate that the vestibular system provides critical compensatory input for stability when other sensory systems are compromised.

### 2.4.3. The Somatosensory System and Postural Control

Proprioceptive control of posture is organized across spinal, brainstem–cerebellar, and cortical levels, where spindle, Golgi tendon organ, joint, and cutaneous inputs are integrated to estimate limb state and to generate both automatic and volitional corrections. With regards to upright stance, proprioceptive feedback supports fine error detection, rapid reflex responses, and higher-order adjustments, with the cerebellum calibrating and refining these actions. When these pathways are compromised (for example after stroke, spinal cord injury, or fatigue), the effective use of proprioceptive information deteriorates, leading to over- or under-corrections. Consistent with impaired sensorimotor integration, EMG coherence studies also report attenuation of higher-frequency activity (>10 Hz) in severe spinal cord injury[48,68,69].

When visual or vestibular cues are degraded, somatosensory channels are adaptively up-weighted to preserve stability. Studies have demonstrated that when individuals stand on a foam surface, they present with significantly increased center of pressure metrics (e.g., increased velocity, displacement, standard deviation, ellipse area)[60,70], indicating impaired postural stability characterized by larger and faster corrective sway to maintain upright balance.

### 2.4.4. Sensory Reweighting

Sensory reweighting is the mechanism by which the central nervous system (CNS) dynamically adjusts reliance on visual, vestibular, and somatosensory inputs to maintain balance. In near-optimal conditions (firm surface, good lighting), somatosensory input typically dominates (≈70%), with vision and vestibular cues providing supporting roles[38,61]. When one channel becomes unreliable (e.g., a compliant surface or low visibility) the CNS down-weights that input and up-weights more reliable modalities, minimizing postural error through continuous evaluation of signal reliability[61,67,71].

Classic perturbation studies by Nashner and colleagues established that postural control is not static and that inappropriate inputs can be rapidly suppressed during sensory conflict[26]. Quantitative modeling further shows that when proprioceptive reliability is degraded by support-surface rotations, reliance on vestibular information increases, providing direct evidence for reweighting[61]. Under visual constraints or low-visibility environment, visual information is absent or degraded; the postural control system correspondingly relies more on vestibular and proprioceptive inputs[72]. These examples illustrate the flexible nature of multisensory integration for posture. Sensory reweighting is the process by which the nervous system maintains adaptive equilibrium by continuously recalibrating the influence of each sensory channel. Subcortical and cortical substrates, including the vestibular nuclei and cerebellum, contribute to these adjustments in sensory integration and reflex gains[64]. Although the overall framework is well supported, how NMF modulates sensory reweighting in tasks of varying postural demands remains insufficiently understood and warrants further study.

### 2.4.5. Sensory Analysis Using Stabilograms

Maintenance of upright balance has been traditionally documented through sway characteristics using measures of amplitude, velocity, path length, and ellipse area of COP displacements[16], which provide information on the extent of spatial fluctuations[35]. While those COP-based outcomes characterize the general neuromechanical response to postural demands[74], these variables primarily summarize kinematic behaviour and do not capture potential alterations in neural regulation, such as shifts between open-loop and closed-loop regulations[73].

To address this limitation, several analytical approaches have been developed to infer the influence of open-loop and closed-loop mechanisms by examining the COP signal at different timescales. Open-loop and closed-loop timescales correspond to exploratory and corrective postural behaviours respectively[75]. Some of the early documented evidence from Collins and DeLuca demonstrated that the closed-loop long term and open-loop short term behaviour of COP displacement can be analyzed through fractal stabilogram diffusion analysis (SDA)[21]. Similarly, the decomposition of COP into two time scale components: rambling and trembling as described by Zatsiorsky and Duarte[76] separates sway into processes reflective of open loop and closed loop[77,78]. Discrete wavelet transform (DWT) decomposition is an ideal method to analyze postural control more in depth, as this approach examines different timescale components through selected high and low frequency ranges using a non-linear time-dependent method to detect irregular and complex interactions. This feature of wavelet decomposition provides insight into the fine-tuned details of the behavioural aspects of postural control, as the frequency intervals go beyond open-loop and closed-loop processes[55] and may provide information into the contribution of specific sensory systems[72].

Studies that have used DWT to analysis open-loop and closed-loop processes in postural control have generally found an overall trend of greater energy distribution in closed-loop frequency intervals compared to open-loop frequency ranges[55,79,80]. During normal quiet standing, spectral energy is predominantly concentrated in long timescales of (0.012–0.049 Hz) compared with short timescales (>1 Hz)[72]. Moderate timescales encompass mid-frequency content (approximately 0.3–1.0 Hz)[81]. Narrow stance quiet standing shows low energy for short timescales and gradually greater contributions of moderate timescales with leveling off at long timescales, reflecting greater contribution of the closed-loop mechanisms compared to open-loop mechanisms[55]. Within the closed-loop frequencies (<1 Hz), the contributions of different sensory systems can be inferred. For example, COP movements below 0.1 Hz are associated with the visual system, those between 0.1 – 0.5 Hz with the vestibular system, and those between 0.5 – 1.0 Hz with the somatosensory system[72]. When vision is removed during narrow stance quiet stance, an overall decrease in energy content of the longer time-scale (<0.1 Hz) bands follows[20,55,80]. When visual sensory information is eliminated, there is also increased energy in the short-term (high frequency) bands, suggesting an exploratory strategy used by the CNS to gain essential sensory information[75,79]. Finally, an isokinetic weighted neck fatigue protocol induced significant increases in long timescales, which

was exacerbated when eyes were closed[20], likely indicative of the postural control system predominantly exhibiting corrective behaviours when faced with NMF. Most DWT studies in postural control address sensory effects during quiet standing (e.g., EO vs. EC) and examine energy across closed- and open-loop bands near 1 Hz, but they seldom integrate fatigue manipulations with varying postural tasks (e.g., forward lean vs. quiet stance) in a single protocol[13,14,72]. To our knowledge, DWT has not been systematically used to characterize fatigue effects across varying postural and sensory conditions, representing a methodological gap concerning task- and context-specific adaptations.

## 2.5. Impact of Neuromuscular Fatigue on Postural Control

NMF can be defined as a transient state characterized by a decline in force-generating capacity of muscle following sustained muscle activity[15]. This decreased capacity to generate force can involve alterations in both central and peripheral sites of the neuromuscular system[16]. The central component of NMF is associated with diminished voluntary activation, while the peripheral component involves localized alterations at or near the fatigued musculature[60,82]. NMF can also lead to reduced proprioceptive acuity[83]. One consequence of fatigue is the disruption of sensorimotor integration, particularly in proprioceptive and exteroceptive feedback pathways[83]. These changes ultimately lead to disruptions in neuromuscular control, which is required for postural stability[15,16].

### 2.5.1. Alterations in Postural Stability and Center of Pressure Dynamics

Maintaining an upright stance requires multisensory input from multiple joints to accurately interpret body position, a process that is compromised following muscle fatigue[84]. These impairments extend to both sensory feedback and the integrative neural response responsible for coordinating postural adjustment responses[19,85]. The fatigue of muscles critical for postural stability, such as the plantar flexors, leads to notable performance deficits, as evidenced by increased sway area and sway velocity. The following paragraph provides a non-exhaustive summary of several studies looking at the effect of fatigue on postural control.

Isometric induced NMF of the ankle muscles has been shown to result in greater sway during quiet standing, with more pronounced effects during more challenging tasks such as unipedal stance[86,89]. The effects of ankle muscle fatigue were further exacerbated when vision was occluded during the postural task[86,87]. Roerdink and collaborators observed increases in range and standard deviation (SD) of COP following fatigue induced by calf raises[88]. Likewise, sway in both mediolateral (ML) and AP directions increased following an isokinetic fatigue task of ankle muscles in a unilateral quiet stance[90]. Similar alterations to the sway velocity were observed following isokinetic contractions of the ankle muscles during a leaning forward task[91]. Fatigue of proximal musculature also compromises balance, with studies demonstrating increased COP velocity in both the frontal and sagittal planes[16,37]. Localized muscle fatigue induced by isometric knee extensors, similarly increased sway velocity with increased effects observed in the anteroposterior axis[9]. A static lunge fatigue protocol caused significant increases in displacement in both ML and AP under eyes closed and eyes open conditions[92]. Similarly, running-induced fatigue caused increased postural instability measured by greater ellipse area during a quiet stance with eyes closed[19] and heightened displacement variance in both ML and AP[85].

Both general and localized NMF can degrade postural stability, with effects typically amplified as task demands increase (e.g., unipedal stance or eyes-closed)[9,16]; however, when compensatory sensory strategies are available, fatigue does not invariably worsen sway[16]. There are instances where postural sway remains unchanged after fatigue or even decreases when individuals maintain visual fixation on a stable target[93,94]. In single-leg stance with eyes open, both total COP path length and mean COP velocity have been shown to decrease following exercise, suggesting a short-term enhancement of postural stability[95]. Similarly, when vision was available, there were no significant increases in COP sway amplitude or variability after fatigue under a feet together or single-leg stance before and after fatigue of the plantar-flexor muscles[96,97].

Wavelet-based decomposition of COP is relatively new in postural control research, and applications under fatigue are still sparse. Emerging studies nonetheless suggest band-specific alterations rather than global changes. For example, reductions in a putative proprioceptive band (1.56–6.25 Hz) have been observed during mental fatigue[98], while selective modulation of ultralow (<0.10 Hz) and moderate (1.56–6.25 Hz) bands has been reported following neck muscle fatigue[20], indicating that wavelet methods can uncover adaptations obscured by aggregate COP metrics.

Building on this growing evidence, the present work applies DWT to examine frequency-resolved effects of localized peripheral fatigue during stance, providing a more detailed view of postural control than is afforded by traditional summary measures.

### 2.5.2. Alterations in Postural Strategies and Muscle Activation Patterns

NMF disrupts the sensory and motor systems, prompting compensatory adjustments in postural control and modifications in motoneuron recruitment patterns[16,99]. For instance, fatigue-induced reductions in torque-generating capacity may lead to altered activation of antagonist muscle groups as a compensatory mechanism[99].

NMF is accompanied by notable changes in muscle coordination and motor strategies. As muscle strength diminishes, the fatigued muscle may no longer be capable of generating the same corrective forces, resulting in balance adjustments that are often slower or of reduced magnitude[16]. To compensate, the neuromuscular system frequently recruits alternative motor strategies. At the ankle, this compensation is expressed as heightened electromyographic (EMG) activity in both agonist and antagonist reflecting the system's attempt to preserve postural stability[16,100]. Donath and collaborators observed increased activation of SOL, GM, and TA but no changes in co-contraction index following a bout of high intensity running[34]. Kennedy *et al.* observed, following isometric muscle fatigue of the ankles, a preparatory co-contraction of the ankle muscles in anticipation of surface pertubances[101]. Contrary to this, Jo and Bilodeau, observed no differences in co-contraction strategies during a static forward leaning task following a similar fatigue protocol[91]. Furthermore, Penedo and colleagues observed no change in CCI following both hip and ankle isokinetic fatigue[102]. Further observed from Kennedy et al. was COP displacement recovery within five minutes post-fatigue, which suggested an involvement of central compensatory mechanisms, as peripheral torque-generating capacity remained largely preserved[101]. Along with the information provided by EMG coherence (next section), this thesis will look at changes in CCI with fatigue under both QS and FL conditions.

### 2.5.3. Changes in Intermuscular Coherence and Neural Coordination

NMF can alter patterns of neural circuitry, potentially affecting both automatic and voluntary levels of muscle activation. Prior evidence looking at these processes through coherence measurements

shows that intermuscular coherence tends to increase among muscles that work synergistically to perform a given task following fatigue. For example, Semmler and collaborators demonstrated that eccentric isometric fatigue of the elbow flexors led to increased coherence between the biceps brachii and brachialis in both the 0–5 Hz and 5–15 Hz frequency bands[10]. Similarly, step-up induced fatigue resulted in increased coherence within the quadriceps femoris group[103]. However, contradictory findings have also been reported; one study observed an overall reduction in coherence between knee extensor synergists following fatigue[104]. During an isometric grasping task, coherence between flexor and extensor muscles increased within the common drive and alpha-band frequency ranges (0–15 Hz)[105]. Conversely, Wang et al. found no significant changes in co-contraction but an increase in coherence between the biceps and triceps during isometric elbow flexion tasks post-fatigue[52], suggesting that the effects of fatigue on intermuscular coherence may vary depending on muscle group, task type, and fatigue protocol. How different EMG coherence frequency bands are influenced by fatigue of ankle dorsi flexors and plantar flexors has yet to be studied, and this is one of the main variables of interest in the present thesis.

# Chapter 3: Methods

## 3.1. Participants

Fourteen healthy young adults (seven females; age 26.4 ± 3.6 years, height 174.2 ± 9.9 cm, and mean body mass 78.8 ± 20.2 kg) volunteered for this study. The required sample size was determined through G* Power Software (version 3.1.9.7) for an analysis of variance (ANOVA) for repeated measures, and was determined to be 11 participants with the following parameters: $\eta^2 = 0.28$, alpha level = 0.05, power = 0.95, correlation among repeated measures = 0.5. The partial eta squared value was chosen based on the effects of fatigue on the alpha band of intermuscular coherence from a previous study of elbow muscles[52]. We recruited 14 young healthy adults (18-35) to account for any losses in data. General exclusion criteria were any individuals presenting with self-reported injuries, degenerative disease, chronic cardiovascular or respiratory system disease, chronic ankle instability or lower back pain, and musculoskeletal conditions. Ethical approval for the study was obtained from the Research Ethics Board at the University of Ottawa (H11-14-23) and from the Bruyère Health Research Ethics Board (M16-08038). All participants were fully informed of the study procedures and provided written consent prior to enrollment.

## 3.2. Postural Tasks

This study aimed at testing the effect of fatigue on EMG and COP variables during two different postural tasks: quiet standing (QS) and a forward leaning (FL) task. Both tasks were performed with eyes opened and closed. A schematic of the experimental setup is shown in Figure 1. Participants first practiced both tasks, then completed two familiarization trials under both eyes-open (EO) and eyes-closed (EC) conditions. They were instructed to maintain a QS posture with their heels about3cm apart and feet externally rotated about 15°, with their arms resting naturally at their sides. Their eyes were fixated on a target located on a wall, about 2.5 m in front of them. For the FL task, participants adopted the same initial stance with arms to the side as during QS, but were instructed to lean forward as far as possible, bending at the ankle and to maintain heel contact with the ground. Once participants were familiar with the tasks, two 30-s trials of each postural task were recorded in a counter-balanced order before and immediately after the fatigue protocol.

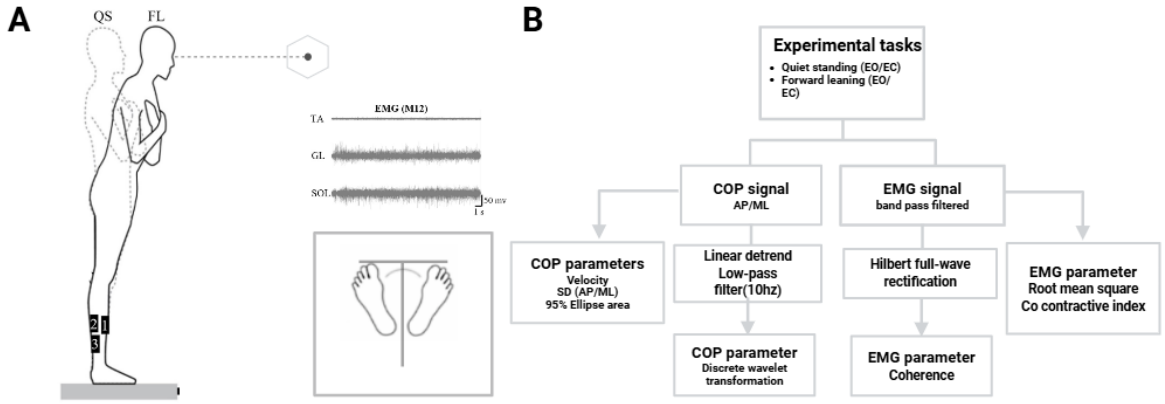


Figure 1: Schematic of the experimental setup **(A)** and flowchart of data analysis plan **(B)**. Participants performed quiet stance and forward-leaning tasks under a butterfly foot position with eyes open and eyes closed. Surface EMG was recorded from the tibialis anterior (TA), gastrocnemius medialis (GM), and soleus (SOL), corresponding to labels 1–3 in panel A. Adapted from [86].

### 3.3. Fatigue Protocol

For the fatigue protocol, participants were seated in a dynamometer chair (Biodex System 3 Pro®, Biodex Medical Systems, Shirley, USA) with the hip flexed to approximately 80°, the legs extended, and both feet secured against a custom footplate set at a 90° angle. Straps were applied at the trunk and waist to restrict movement and isolate torque generation to the ankle joint. Baseline peak torque for both plantarflexion (PF) and dorsiflexion (DF) was established using two maximal isometric voluntary contractions (MVCs) in each direction, with a 1 min rest period between contractions. Fatigue was induced through alternating maximal isometric contractions of the plantarflexors (for 6 s) and dorsiflexors (for 2 s), paced using a metronome application to ensure consistent timing across participants. The protocol was continued until participants failed to sustain 50% of their MVC for the majority of the contraction duration across both movement directions. The respective PF and DF contraction duration were chosen based on differing resistance to fatigue as described in previous studies[91,101]. The target torque was disclosed only to the investigators, as revealing this information could have prevented participants from exerting maximal effort during the fatiguing exercise. Continuous verbal encouragement was provided throughout the protocol.

### 3.4. Data acquisition

COP data was acquired using an AMTI AcuGait force platform (Watertown, MA, USA) at a sampling frequency of 100 Hz. Electromyographic (EMG) signals were recorded using bipolar surface electrodes (width: 1 mm, length: 10 mm, and center-to-center interelectrode distance: 10 mm; DE-2.1, Delsys Inc., Boston, MA, USA). These EMG signals were amplified (×1,000; common mode rejection ratio: 92 dB; channel frequency response: 20–450 Hz) and recorded at a sampling rate of 2,020 Hz. Recording electrodes were placed unilaterally on the dominant leg, determined by a single self-report question and a simple motor task (ball rolled to the participant's feet). Electrode placement followed SENIAM recommendations over the soleus (SOL), tibialis anterior (TA), and gastrocnemius medialis (GM). The reference electrode was placed on the patella of the same leg. Participants were asked to wear appropriate clothing that would not obstruct EMG electrode placement sites. After the electrodes were placed, a quality check was performed to ensure EMG signal quality. All raw data were stored locally on an offline desktop computer using Spike2 software (Cambridge Electronic Design).

### 3.5. Data Processing

#### 3.5.1. Muscle activation and co-contraction

The root mean square (RMS) amplitude (Equation (1)) of the EMG signals from MG, SOL and TA was first calculated over each 30-s trial in all conditions (QS/FL and EO/EC). Co-contraction was quantified using the method proposed by Ruduloph[106], where EMG RMS amplitude for a given 30-s trial was first normalized to the EMG RMS value (over a 1-s window) obtained during the highest plantarflexion (for GM and SOL) or dorsiflexion (for TA) MVC[52].

$$RMS = \sqrt{\frac{1}{N}\sum_{i=1}^{N} x_i^2} \tag{1}$$

Co-contraction of normalized EMG RMS signals between intermuscular pairs (GM-TA and SO-TA) was assessed using the following equation:

$$CCI = \frac{EMG_{low}}{EMG_{high}} * \ (EMG_{low} + \ EMG_{high}) \tag{2}$$

where $EMG_{low}$ and $EMG_{high}$represent the muscle of the higher and lower muscle activity of two different muscles in a given time period[32]. A high co-contraction index value represents a high level of activation of both muscles indicative of high co-contraction[106].

### 3.5.2. Coherence

For the intermuscular coherence analysis, the full-wave rectified (via Hillbert transform[44]) surface EMG signals for each 30-s trial of each subject were used. The purpose of rectification is to improve the detection of motor unit synchronization patterns by emphasizing frequency components in the 0-30 Hz range that reflect common neural drive, while minimizing the contribution of high-frequency spectral content associated with motor unit action potential waveform properties[45,107]. The coherence was calculated for a segment length of 1024 samples with 50 % overlap, using a Hanning window[108] in Jupyter labs using the NumPy, pandas, SciPy, and seaborn libraries. The magnitude squared coherence $C_{xy}(f)$ between two EMG was obtained from agonist-agonist and agonist-antagonist intermuscular pairs using the following equation:

$$C_{xy}(f) = \frac{\left|S_{xy}(f)\right|^2}{S_{xx}(f) * S_{yy}(f)} \tag{3}$$

where $C_{xy}(f)$ is the ratio of the squared magnitude of the cross-spectra $S_{xy}(f)$ and the product of the auto-spectra of each signal $S_{xx}(f) * S_{yy}(f)$. Both trials for a given task/condition were averaged.

### 3.5.3. Stabilometric measurements

Standard COP variables were calculated for each 30-s trial: sway amplitude (COP standard deviation) in AP and ML directions, velocity in AP and ML directions and the area of the 95% confidence ellipse, using the following equations:

$$COP\sigma_{AP} = \sqrt{\frac{1}{N-1}\sum_{i=1}^{N}(x_i - \bar{x})^2} \tag{4}$$

$$COP\sigma_{ML} = \sqrt{\frac{1}{N-1}\sum_{i=1}^{N}(y_i - \bar{y})^2} \quad (5)$$

$$V_{AP} = \frac{1}{T}\sum_{i=2}^{N}\frac{|x_i - x_{i-1}|}{\Delta t} \quad (6)$$

$$V_{ML} = \frac{1}{T}\sum_{i=2}^{N}\frac{|y_i - y_{i-1}|}{\Delta t} \quad (7)$$

$$Area_{95\%} = 2\pi * \frac{N-1}{N-2} * F_{0.95,2,N-2} * \sqrt{RMS_{ML}^2 * RMS_{AP}^2 - COV^2} \quad (8)$$

### 3.5.4. Discrete Wavelet Transform

A discrete wavelet transform (DWT) is a method of signal analysis used to characterize the spatial and temporal synchronization of COP displacements[109]. The DWT is the break down of a signal with multiple frequency components (mother wavelet) into smaller timeseries with different time scales and transitions[55,110]. This analysis allows for the identification of the energy contribution of different frequency components, which can reflect, amongst other things, open-loop and closed-loop processes. The wavelet coefficient (WC) at time scale *a* and time instant *b* represents the conversions of these variables into a two-dimensional real space, providing insight into the contribution of different sensory inputs, using the following equation:

$$WC = \int_{-\infty}^{+\infty} s(t)\psi_{a,b}^{*}(t)dt \quad (9)$$

where s(t) represents the time series signal, * represents the complex conjugate. $\psi$ represents the child wavelets function obtained from the mother wavelet from the following equation:

$$\psi_{a,b}(t) = \frac{1}{\sqrt{a}}\psi(\frac{t-b}{a}) \quad (10)$$

The child wavelet is a function of time of timescale $t_a$ localized near the time instant *b*. In discrete wavelet transform both the timescale $t_a$ and time instant b become discrete such that a and b are integers, $a = 2^j \quad b = 2^j k$. Where $j = 1, \dots, J$ represent discrete levels of timescales at ranges at

each level $j$ of $t_j = \left\{\frac{2^{2^{(j-1)}}}{f_{sampling}}, \frac{2^{2^j}}{f_{sampling}}\right\}$ and $k = 0, \ldots, K(j)$. Prior to wavelet transform, the raw COP signal was linearly detrended to remove slow drift and DC bias[111] and low pass filtered (10 Hz) to attenuate high frequency noise while preserving all relevant physiological sway related responses[112]. A maximal overlap discrete wavelet transform was obtained using R studio software with the waveslim package[113]. Eleven (11) discrete levels were obtained using a la8 filter. From those, the following frequency intervals were analyzed for contributions of open-loop (>1 Hz) and closed-loop processes (<1 Hz) to elucidate the contribution of different sensory inputs [72]:

- 0-0.1 Hz; visual system (closed-loop)
- 0.1-0.5 Hz; vestibular system (closed-loop)
- 0.5-1 Hz; somatosensory system (closed-loop)
- 1-10 Hz (open-loop)

The energy content at each frequency level (j) was calculated using the following:

$$E_i\% = \frac{\sum_j (c_{ij})^2}{\sum_k \sum_j (c_{ij})^2}\ 100\% \tag{11}$$

where c is the decomposed frequency detail, including approximation. From this analysis, we were able to compare to what extent the open-loop and closed-loop processes contribute to postural stability under fatigued conditions based on the frequency ranges and their respective energy contribution.

### 3.6. Statistical analyses

Statistical analyses were performed in R (version 4.x; R Core Team, Vienna, Austria). Coherence values and wavelet-derived energy fractions are bounded between 0 and 1 (coherence) or 0 and 100 (wavelet), and thus violate normality assumptions required for parametric testing. Similar to previous studies, we calculated z-transformed coherence over the frequency ranges from magnitude-squared coherence values prior to statistical analyzes[5,24,49,114]. This stabilizes variance to prevent any violations to normal distribution of data. Discrete wavelet transformation data were logit-transformed prior to statistical analysis (ANOVAs and post hoc tests). Statistical tests were performed in the transformed space for coherence and wavelet analysis. Shapiro-Wilk and

Levene's tests were conducted to verify normality and variance homogeneity assumptions before all statistical and signal processing analyses. Three-way repeated measures analysis of variance (ANOVA) were employed to examine the main and interaction effects of fatigue state (pre-fatigue vs. post-fatigue), task condition (quiet standing vs. forward leaning), and visual condition (eyes open vs. eyes closed) on outcome measures (1) $COP_{vel}$, (2) $COP_{SD}$, (3) confidence ellipse area, (4) $EMG_{RMS}$, and (5) co-contraction index using aov_afex function in the afex package. Three-way repeated-measures ANOVA were used to examine the main effects and interactions of fatigue state (pre-fatigue vs. post-fatigue), task condition (quiet standing vs. forward leaning), and frequency band for (6) logit transformed wavelet of $COP_D$ and (7) z-score coherence using aov_afex function in the afex package. The assumption of sphericity was assessed using Mauchly's test for each within-subject factor and interaction. Sphericity was evaluated and when the assumption of sphericity was violated ($p < .05$), Greenhouse–Geisser (GG) corrections were applied to the degrees of freedom, and the corrected *p*-values are reported with effects with more than two levels. Generalized eta squared (GES) was calculated as a measure of effect size for each main effect and interaction. Pairwise post-hoc comparisons with Bonferroni correction were performed to assess fatigue-related changes within each postural task and frequency band when significant interactions were present. Pre–Post effects were evaluated using either a one-way repeated-measures ANOVA with factor Fatigue (Pre, Post) or an equivalent paired t-test, in both cases using the repeated-measures error term. Additionally, Pearson product-moment correlation coefficients were calculated to assess the associations between fatigue-induced changes in electromyographic (EMG) coherence and corresponding changes in Discrete wavelet transformation for each task.

# Chapter 4: Results

The results presented here focus primarily on the effects of fatigue, reflecting the central aim of this thesis to examine how localized muscular fatigue alters postural control and neuromuscular coordination. All statistical analyses and post hoc comparisons were therefore structured to evaluate fatigue-related changes across conditions and tasks, with secondary emphasis on task- and vision-dependent interactions (some results provided in the appendix).

## 4.1. EMG Results

Table 1 summarizes the mean duration of each fatigue bout, with an expected decline in time to task failure across successive bouts.

Table 1: Duration of each fatigue bout (s). Values are mean ± SD across participants. Duration is the elapsed time to the end of each bout.

| | Fatigue Bout 1 | Fatigue Bout 2 | Fatigue Bout 3 | Fatigue Bout 4 |
|---|---|---|---|---|
| *Duration (s)* | 129.6s ± 36.3 | 88.7s ± 20.9 | 98.1s ± 46.2 | 87.9s ± 40.8 |

Figures 2 and 3 display the raw EMG and COP recordings from a representative participant during the QS and FL trials, illustrating the baseline signal features and differences between postural conditions.

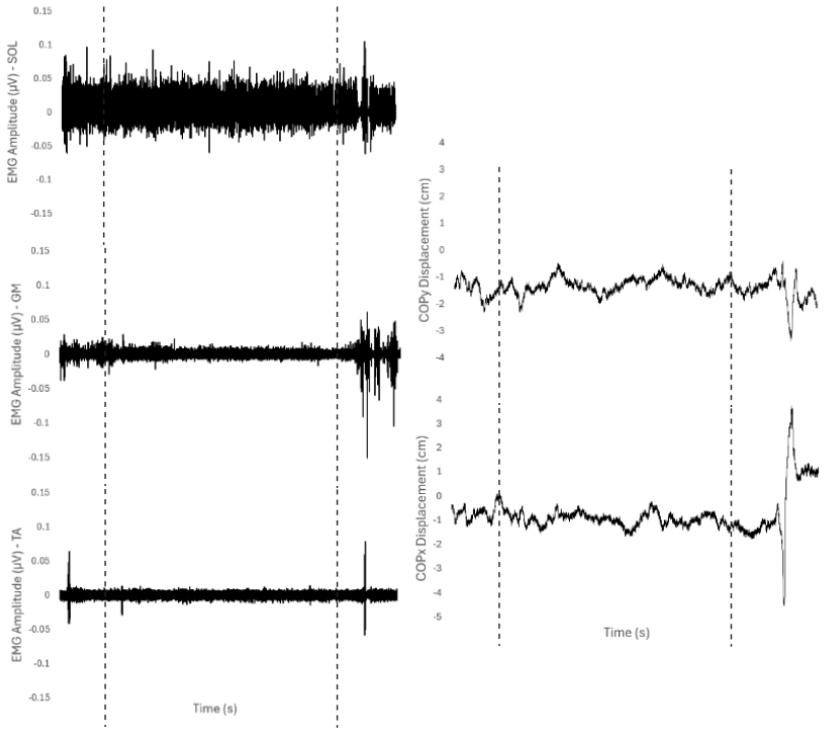


Figure 2: Raw electromyographic activity of muscle groups during quiet standing trial from Subject #04. Between dashed lines mark the 30 s window used for analysis for the trial.

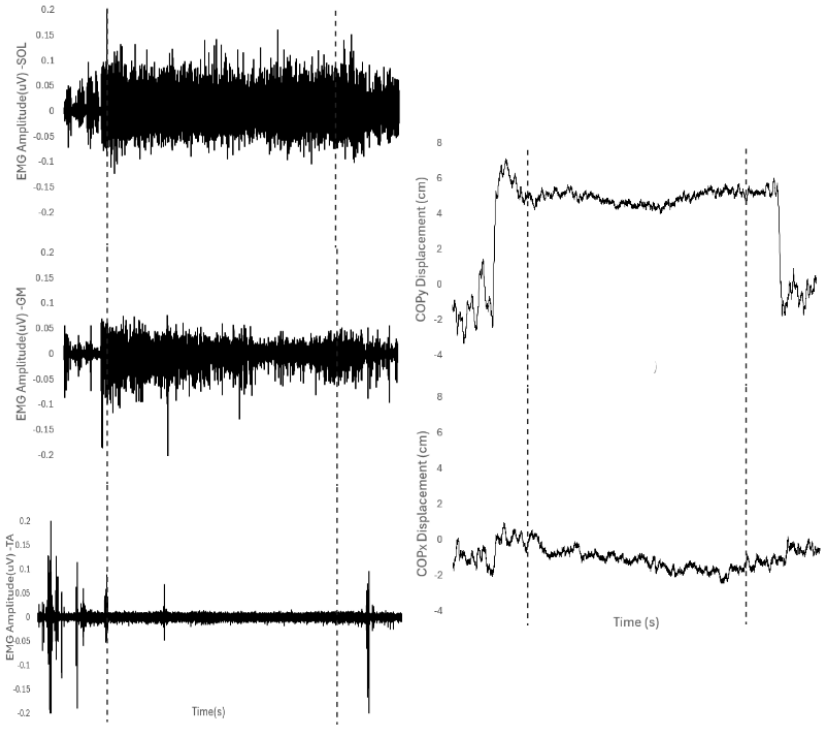


Figure 3: Raw electromyograph activity of muscle groups during forward leaning trial from Subject #04. Between dashed lines mark the 30 s window used for analysis for the trial.

### 4.1.1. EMG Amplitude: Root Mean Square (RMS) and Co-Contraction Index

For soleus (SOL) and tibialis anterior (TA) RMS amplitude, there was no main effect of fatigue and no fatigue-related interactions (Table 2). In contrast, gastrocnemius medialis (GM) showed a main effect of fatigue as well as fatigue × task and fatigue × vision interactions. Post-hoc comparisons of mean differences in GM RMS amplitude indicated a decrease in EMG amplitude after fatigue across conditions, but reaching significance only for the FLEO condition (8.76%; Table 3). In general, EMG amplitude was higher during forward lean than quiet standing across all three muscles in both eyes open and EC conditions, yielding significant main effects of task. Moreover, EMG amplitude was generally higher with eyes closed than with EO (Tables 4 & 5). See Figure A1 in the appendix for normalized RMS EMG amplitude values across conditions.

Table 2: Results of the three-way repeated-measures ANOVA examining the effects of fatigue, postural task, and vision on muscle activation of SOL, GM, and TA.

| Muscle | Effect | df | F | p | Muscle | F | p | Muscle | F | p |
|---|---|---|---|---|---|---|---|---|---|---|
| *SOL* | *Fatigue* | 1,10 | 0.076 | 0.788 | *GM* | 5.693 | **0.0382*** | *TA* | 1.239 | 0.2917 |
| | *Task* | 1,10 | 51.305 | **<0.0001***** | | 25.423 | **0.0005**** | | 7.637 | **0.02*** |
| | *Vision* | 1,10 | 2.488 | 0.1458 | | 13.306 | **0.0045**** | | 3.551 | 0.0889 |
| | *Fatigue*Task* | 1,10 | 0.908 | 0.363 | | 13.617 | **0.0042**** | | 3.693 | 0.0836 |
| | *Fatigue*Vision* | 1,10 | 0.36 | 0.5621 | | 9.843 | **0.0106*** | | 1.027 | 0.3349 |
| | *Task*Vision* | 1,10 | 0.43 | 0.5268 | | 2.013 | 0.1864 | | 0.809 | 0.3894 |
| | *Fatigue*Task*Vision* | 1,10 | 1.35 | 0.2723 | | 0.727 | 0.4138 | | 0.132 | 0.7237 |

** p < .05; **p < .01; ***p < .001*

Table 3: Post-hoc paired comparisons (Post − Pre) of EMG amplitude by condition following the ANOVA GM. Values are means; mean differences are reported as Post − Pre and difference of SE, t(df), and p reported.

| Muscle | Condition | Pre Mean | Post Mean | Mean Diff (Post-Pre) | SE Diff | t(df) | p |
|---|---|---|---|---|---|---|---|
| GM | QSEO | 12.8221 | 9.5034 | -4.1189 ± 3.8753 | 3.8753 | -1.0629(12) | 0.6175 |
| | FLEO | 24.7503 | 22.5816 | -4.5124 ± 1.7531 | 1.7531 | -2.574(13) | **0.0462** |
| | QSEC | 10.4883 | 6.3695 | -3.3186 ± 4.1214 | 4.1214 | -0.8052(13) | 0.8703 |
| | FLEC | 24.4862 | 19.9738 | -2.1686 ± 1.2656 | 1.2656 | -1.7135(13) | 0.2207 |

Table 4: Paired t-tests comparing RMS muscle activation between quiet stance (QS) and forward leaning (FL) under eyes-open conditions.

| Muscle | Fatigue | QS Mean ± SE | FL Mean ± SE | Mean Diff (FL–QS) | SE Diff | t(df) | p |
|---|---|---|---|---|---|---|---|
| *SOL* | Pre | 8.1414 ± 1.0763 | 18.4700 ± 1.5483 | 10.3285 | 1.1281 | 9.1559(12) | **<.0001***** |
| | Post | 8.2012 ± 0.9317 | 18.2097 ± 1.1167 | 10.0085 | 0.97 | 10.3185(12) | **<.0001***** |
| *GM* | Pre | 10.4883 ± 3.7011 | 23.5664 ± 4.3183 | 13.078 | 5.2295 | 2.5008(12) | 0.0836 |
| | Post | 6.3695 ± 1.3294 | 18.8827 ± 3.5734 | 12.5132 | 2.9635 | 4.2225(12) | **0.0036*** |
| *TA* | Pre | 2.7126 ± 0.3767 | 4.9034 ± 1.1464 | 2.1908 | 1.1401 | 1.9215(10) | 0.2508 |
| | Post | 2.6796 ± 0.2661 | 4.4347 ± 0.6682 | 1.7551 | 0.6329 | 2.7732(10) | 0.059 |

** p < .05; **p < .01; ***p < .001*

Table 5: Paired t-tests comparing RMS muscle activation between quiet stance (QS) and forward leaning (FL) under eyes-closed conditions.

| Muscle | Fatigue | QS Mean ± SE | FL Mean ± SE | Mean Diff (FL–QS) | SE Diff | t(df) | p |
|---|---|---|---|---|---|---|---|
| *SOL* | Pre | 8.4893 ± 1.1034 | 18.5999 ± 1.3804 | 10.1106 | 1.0795 | 9.366(13) | **<.0001*** ** |
| | Post | 9.2483 ± 1.1681 | 18.3427 ± 1.1496 | 9.0943 | 0.7484 | 12.1516(13) | **<.0001*** ** |
| *GM* | Pre | 12.8221 ± 3.8260 | 34.6591 ± 10.0041 | 21.837 | 6.3143 | 3.4584(13) | **0.0127*** |
| | Post | 9.5034 ± 2.0317 | 22.5816 ± 4.0555 | 13.0782 | 3.1659 | 4.131(13) | **0.0035*** |
| *TA* | Pre | 2.8892 ± 0.4038 | 5.9809 ± 1.1856 | 3.0916 | 1.1047 | 2.7986(11) | 0.052 |
| | Post | 2.9453 ± 0.3850 | 4.5975 ± 0.6241 | 1.6522 | 0.6026 | 2.7417(11) | 0.0575 |

** p < .05; **p < .01; ***p < .001*

A three-way repeated-measures ANOVA on CCI revealed a main effect of task on the SOL-TA pair (Table 6). No other main effects or interactions emerged; therefore, post hoc analyses were not conducted.

Table 6: Results of the repeated-measures ANOVA on the co-contraction index (CCI). Rows list the tested effects (Fatigue, Postural Task, Vision, and their interactions). Columns report the denominator degrees of freedom (df), the F statistic for each effect, and the corresponding two-tailed p-value.

| Muscles | Effect | df | F | p | Muscles | df | F | p |
|---|---|---|---|---|---|---|---|---|
| *SOL-TA* | Fatigue | 1,10 | 1.2271 | 0.2939 | *GM-TA* | 1,10 | 0.6675 | 0.4329 |
| | Task | 1,10 | 5.0219 | **0.0489*** | | 1,10 | 3.0535 | 0.1111 |
| | Vision | 1,10 | 2.7255 | 0.1298 | | 1,10 | 1.3794 | 0.2674 |
| | Fatigue:Task | 1,10 | 4.2183 | 0.0671 | | 1,10 | 2.3788 | 0.154 |
| | Fatigue:Vision | 1,10 | 1.7939 | 0.2101 | | 1,10 | 2.3593 | 0.1556 |
| | Task:Vision | 1,10 | 0.1536 | 0.7034 | | 1,10 | 0.4448 | 0.5199 |
| | Fatigue:Task:Vision | 1,10 | 0.0187 | 0.8939 | | 1,10 | 0.0641 | 0.8053 |

** p < .05; **p < .01; ***p < .001*

Figure 4 illustrates that co-contraction levels for SOL-TA were consistently higher during forward lean compared to quiet stance and greater under eyes-closed conditions, indicating increased muscle co-activation with elevated postural demands. Across both pre- and post-fatigue blocks, forward lean exceeded quiet stance and eyes closed exceeded eyes open, with overlapping but generally smaller SEM bars post-fatigue, suggesting modest attenuation yet preservation of the task- and vision-related patterns. Overall, the figure demonstrates that the characteristic task- and vision-dependent differences in SOL–TA co-contraction were largely maintained following fatigue.

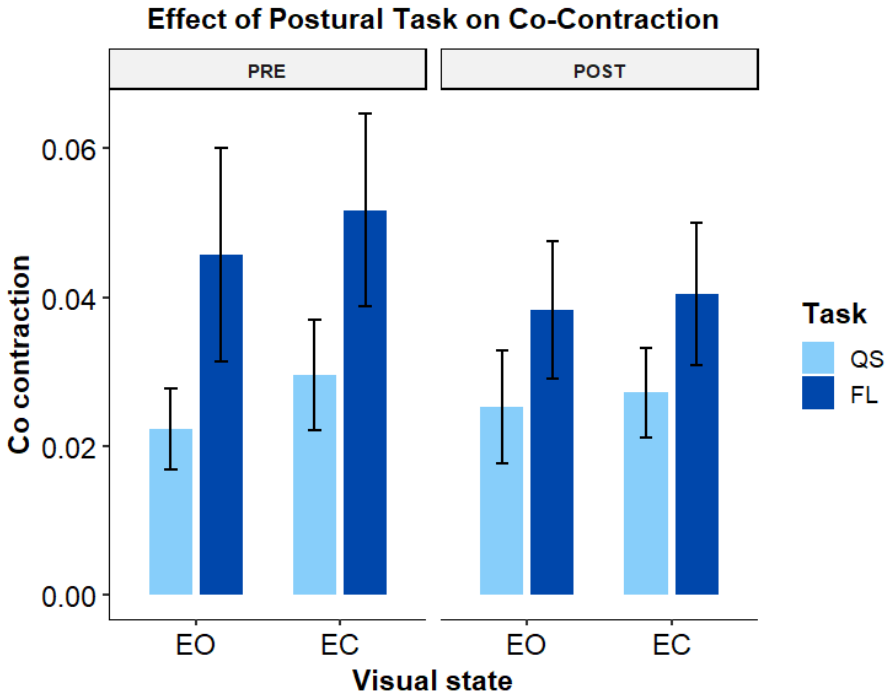


Figure 4: Effect of postural task and visual condition on muscle co-contraction before and after fatigue for SOL-TA. Mean (± SEM) Co-contraction Index (CCI) values are shown for (QS, light blue) and (FL, dark blue) tasks under eyes-open EO and EC conditions, both pre- and post-fatigue.

### 4.1.2. EMG Coherence

Figures 5 and 6 show the EMG coherence between SOL–GM, GM–TA and SOL–TA from participant #6, obtained during a quiet standing and forward leaning trial performed before fatigue. During quiet stance, agonist–agonist (AG–AG) coherence peaked in the low-frequency range (~0–6 Hz). Under forward lean, AG–AG coherence declined in peak amplitude at low frequencies but spread over a wider band, while AG–ANT coherence increased relative to quiet stance. Overall, the task-dependent changes in coherence provide a representative example of how postural demands shape the organization of intermuscular coordination, a pattern explored in detail in the group-level analyses presented below.

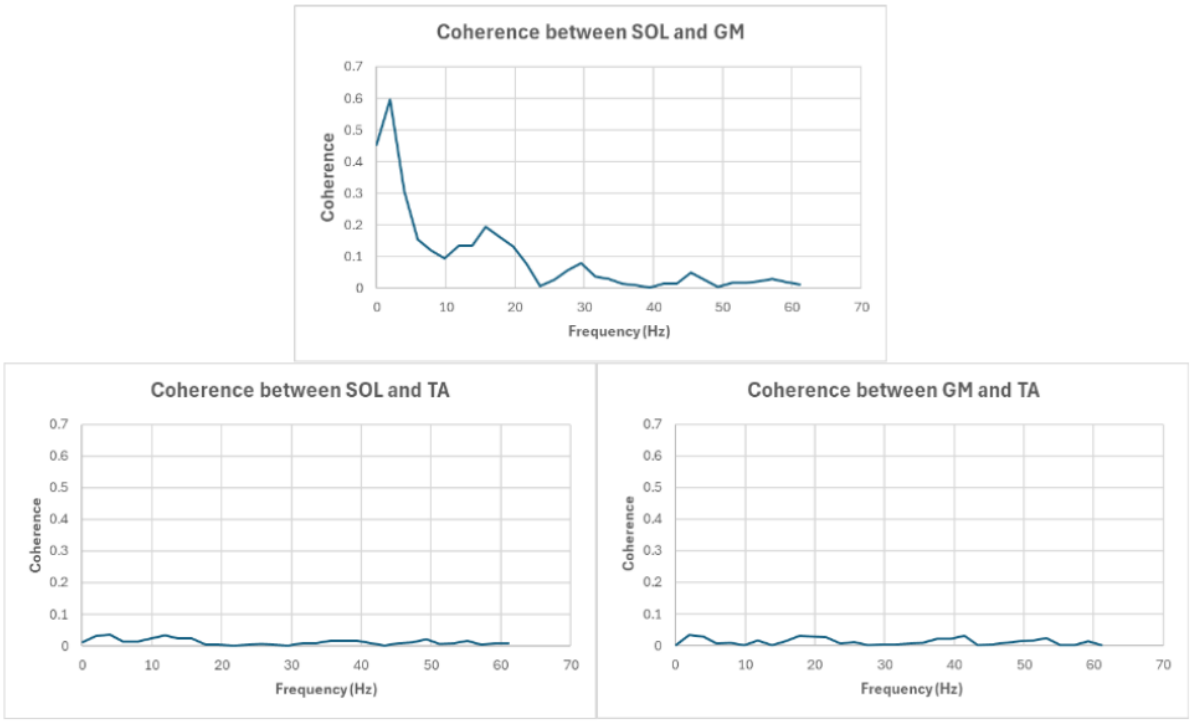


Figure 5: Quiet standing coherence spectrum from Subject #6.

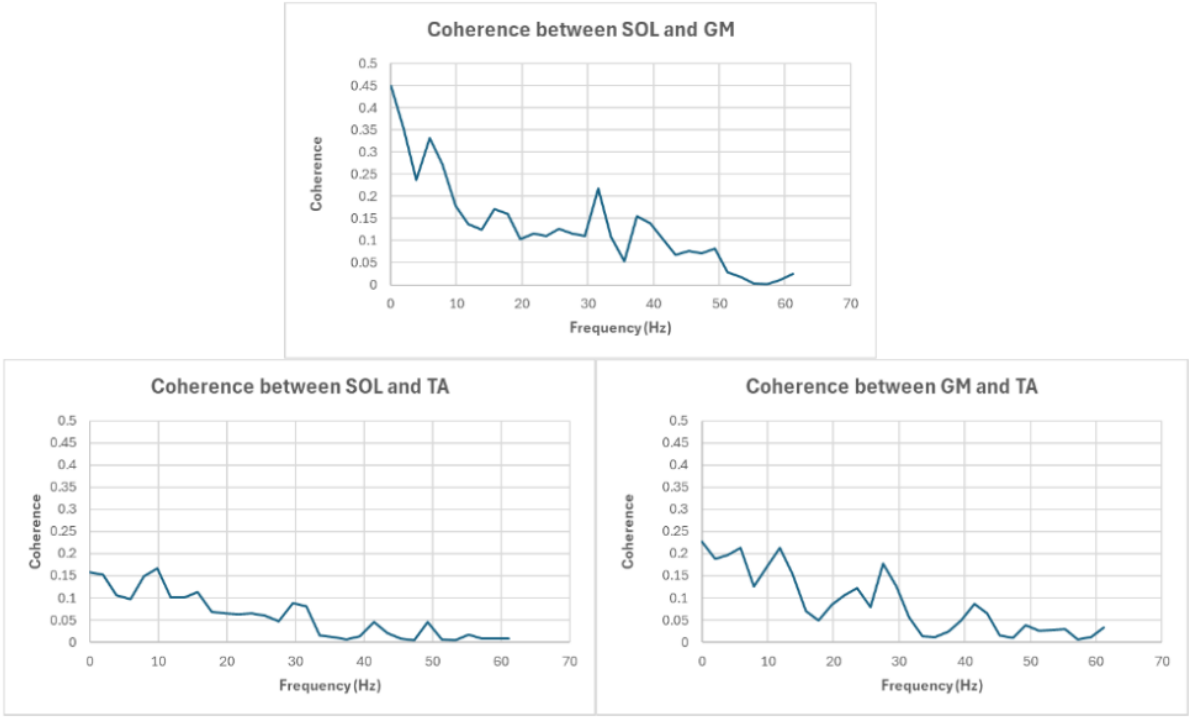


Figure 6: Forward lean coherence spectrum from Subject #6.

Figure 7 shows box plots of AG–AG (SOL-GM) coherence across the different conditions. Table 7 shows the results of the 3-way ANOVAs performed for both EO and EC conditions. For EO AG-AG coherence, neither Fatigue nor Postural Task showed a main effect. In contrast, Frequency Band showed a significant effect. There were significant interactions observed for Fatigue × Task, Fatigue × Frequency band, and Task × Frequency Band (see Figure A2 in the appendix). For EC, there were no main effects of Fatigue or Task. Significant interactions were observed for Fatigue × Frequency band and Task × Frequency band. The three-way interaction was not significant for either vision condition. Post-hoc analyses demonstrated that the fatigue effect was task- and band-dependent. As summarized in Table 8 and illustrated in Figure 7, a significant pre–post increase in SOL-GM coherence emerged specifically in the Mid and High frequency bands, for the FLEC condition. The Mid band (5.92–15.78 Hz) showed an increase in coherence from 0.382 ± 0.0512 to 0.391 ± 0.0624 (Bonferroni-adjusted p = 0.0029, **). In the High band (17.75–39.45 Hz), coherence increased from 0.277 ± 0.0360 to 0.291 ± 0.0383 (Bonferroni-adjusted p = 0.032, *). No Bonferroni-corrected effects were observed in the Low band. Collectively, the results demonstrate that coherence responses to fatigue were highly condition-dependent, with meaningful changes restricted to forward lean under eyes-closed conditions and confined to the Mid and High frequency bands.

Table 7: Results of the three-way repeated-measures ANOVAs examining the effects of fatigue, postural task, and frequency band on Fisher z-transformed SOL–GM coherence for both eyes-open and eyes-closed conditions. Degrees of freedom and p values are Greenhouse–Geisser–adjusted where applicable; generalized eta squared (GES) is reported as the effect-size metric. Mean squared error (MSE) terms are reported per effect in the table. Sample size after exclusions due to missing data; n = 13 (df for the Condition main effect = 1,12).

| Effects | Eyes-open (AG-AG) SOL-GM | | | | | Eyes-closed (AG-AG) SOL-GM | | | | |
|---|---|---|---|---|---|---|---|---|---|---|
| | df(GG) | MSE | F | p-value | ges | df(GG) | MSE | F | p-value | ges |
| *Fatigue* | 1, 12 | 0.02 | 1 | 0.337 | 0.004 | 1, 13 | 0.03 | 0.67 | 0.429 | 0.002 |
| *Postural Task* | 1, 12 | 0.01 | 0.93 | 0.353 | 0.002 | 1, 13 | 0.03 | 2.39 | 0.146 | 0.007 |
| *Frequency Band* | 1.22, 14.70 | 0.05 | 21.83 | **<.001*** ** | 0.166 | 1.32, 17.12 | 0.07 | 31.54 | **<.001*** ** | 0.228 |
| *Fatigue ×Postural Task* | 1, 12 | 0 | 12.46 | **0.004** ** | 0.004 | 1, 13 | 0.01 | 2.25 | 0.158 | 0.003 |
| *Fatigue × Frequency Band* | 1.28, 15.33 | 0.01 | 3.6 | **<.001*** ** | 0.056 | 1.17, 15.27 | 0.02 | 18.75 | **<.001*** ** | 0.045 |
| *Postural Task × Frequency Band* | 1.89, 22.66 | 0 | 20.13 | **0.046*** | 0.002 | 1.17, 15.25 | 0.01 | 4.58* | **0.044*** | 0.005 |
| *Fatigue × Postural Task × Frequency Band* | 1.49, 17.91 | 0 | 1.37 | 0.272 | 0.001 | 1.23, 16.05 | 0.01 | 0.02 | 0.932 | <.001 |

** p < .05; **p < .01; ***p < .001*

Table 8: Repeated-measures comparison of Pre vs Post SOL–GM (AG–AG) z-coherence by frequency band and postural task. Values are mean ± SE for Pre and Post; the two-level RM one-way ANOVA (Pre vs Post) is reported for each cell. p-values are Bonferroni-adjusted within task across bands (Low 0–4 Hz, Mid 6–16 Hz, High 17–40 Hz).

| AG-AG (SOL-GM) | *Main effect - Fatigue* | | | | | | |
|---|---|---|---|---|---|---|---|
| | F(df) | Pre (Mean ± SE) | Post (Mean ± SE) | MSE | p | p (Bonferroni-corr.) | GES |
| **QSEO** | | | | | | | |
| *Low (0–3.94 Hz)* | 0.561(13) | 0.599 ± 0.0717 | 0.623 ± 0.0632 | 0.0773 | 0.206 | 0.617 | 0.007 |
| *Mid (5.92–15.78 Hz)* | 17.93(13) | 0.448 ± 0.0604 | 0.554 ± 0.0663 | 0.0423 | 0.741 | 1.000 | 0.001 |
| *High (17.75–39.45 Hz)* | 8.877(13) | 0.388 ± 0.0460 | 0.456 ± 0.0544 | 0.0180 | 0.273 | 0.818 | 0.003 |
| **QSEC** | | | | | | | |
| *Low (0–3.94 Hz)* | 0.133(14) | 0.786 ± 0.0815 | 0.759 ± 0.1042 | 0.0489 | 0.154 | 0.461 | 0.006 |
| *Mid (5.92–15.78 Hz)* | 1.944(14) | 0.453 ± 0.0582 | 0.502 ± 0.0649 | 0.0445 | 0.026 | 0.078 | 0.028 |
| *High (17.75–39.45 Hz)* | 1.807(14) | 0.335 ± 0.0401 | 0.359 ± 0.0431 | 0.0273 | 0.262 | 0.786 | 0.007 |
| ***FLEO*** | | | | | | | |
| *Low (0–3.94 Hz)* | 2.296(14) | 0.472 ± 0.0572 | 0.504 ± 0.0609 | 0.123 | 0.721 | 1.000 | 0.002 |
| *Mid (5.92–15.78 Hz)* | 6.315(14) | 0.419 ± 0.0512 | 0.488 ± 0.0612 | 0.053 | 0.187 | 0.560 | 0.012 |
| *High (17.75–39.45 Hz)* | 1.375(14) | 0.372 ± 0.0385 | 0.399 ± 0.0491 | 0.024 | 0.202 | 0.606 | 0.006 |
| **FLEC** | | | | | | | |
| *Low (0–3.94 Hz)* | 1.791(14) | 0.636 ± 0.0687 | 0.593 ± 0.0847 | 0.064 | 0.467 | 1 | 0.002 |
| *Mid (5.92–15.78 Hz)* | 0.115(14) | 0.382 ± 0.0512 | 0.391 ± 0.0624 | 0.056 | <0.001 | **0.0029**** | 0.051 |
| *High (17.75–39.45 Hz)* | 1.322(14) | 0.277 ± 0.0360 | 0.291 ± 0.0383 | 0.036 | 0.011 | **0.032*** | 0.034 |

** p < .05; **p < .01; ***p < .001*

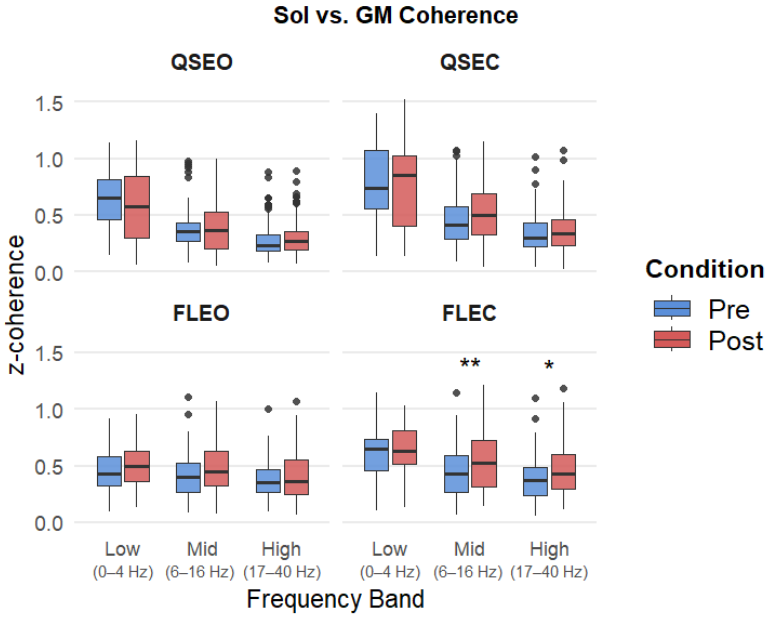


Figure 7: Boxplots of SOL–GM (agonist–agonist) z-coherence by postural task (QSEO, QSEC, FLEO, FLEC) and frequency band [Low (0–4 Hz), Mid (6–16 Hz), High (17–40 Hz)], comparing Pre (blue) and Post (red) fatigue. Boxes show the interquartile range with median lines; whiskers indicate 1.5× IQR and points are outliers. Asterisks mark Bonferroni-adjusted Pre–Post differences within each task across the three bands ($p < .05$ = *, $p < .01$ = **).

For the agonist-antagonist pairs, both SOL-TA and GM-TA coherence showed a significant effect of fatigue ($p < .021$; Table 9 & 11), but no interactions. An increase in coherence was observed post-fatigue, and was not dependent on task, frequency band or vision conditions (Tables 9 and 10, Figures 8 and 9). This pattern suggests a generalized enhancement of shared neural drive between agonist and antagonist muscles following fatigue.

Table 9: Results of the three-way repeated-measures ANOVAs examining the effects of fatigue, postural task, and frequency band on Fisher z-transformed SOL-TA coherence for both eyes-open and eyes-closed conditions. Degrees of freedom and p values are Greenhouse–Geisser–adjusted where applicable; generalized eta squared (GES) is reported as the effect-size metric. Mean squared error (MSE) terms are reported per effect in the table. Sample size after exclusions due to missing data; n = 13 (df for the Condition main effect = 1,12).

| Effects | Eyes-open (AG-ANT) SOL-TA | | | | | Eyes-closed (AG-ANT) SOL-TA | | | | |
|---|---|---|---|---|---|---|---|---|---|---|
| | df(GG) | MSE | F | p-value | ges | df(GG) | MSE | F | p-value | ges |
| *Fatigue* | 1, 10 | 0.01 | 29.93*** | **<.001** | 0.301 | 1, 11 | 0.01 | 23.02*** | **<.001*** ** | 0.131 |
| *Postural Task* | 1, 10 | 0 | 1.9 | 0.198 | 0.004 | 1, 11 | 0 | 12.72** | **0.004** ** | 0.032 |
| *Frequency Band* | 1.37, 13.70 | 0.01 | 1.31 | 0.287 | 0.014 | 1.18, 13.02 | 0.02 | 1.16 | 0.313 | 0.013 |
| *Fatigue ×Postural Task* | 1, 10 | 0.01 | 0.14 | 0.718 | 0.002 | 1, 11 | 0.01 | 1.62 | 0.23 | 0.004 |
| *Fatigue × Frequency Band* | 1.37, 13.69 | 0 | 0.98 | 0.367 | 0.005 | 1.64, 18.02 | 0 | 0.9 | 0.407 | 0.002 |
| *Postural Task × Frequency Band* | 1.78, 17.75 | 0 | 0.98 | 0.385 | 0.002 | 1.58, 17.37 | 0 | 1.19 | 0.316 | 0.002 |
| *Fatigue × Postural Task × Frequency Band* | 1.48, 14.83 | 0 | 0.43 | 0.6 | 0.002 | 1.69, 18.58 | 0 | 0.72 | 0.476 | <.001 |

** p < .05; **p < .01; ***p < .001*

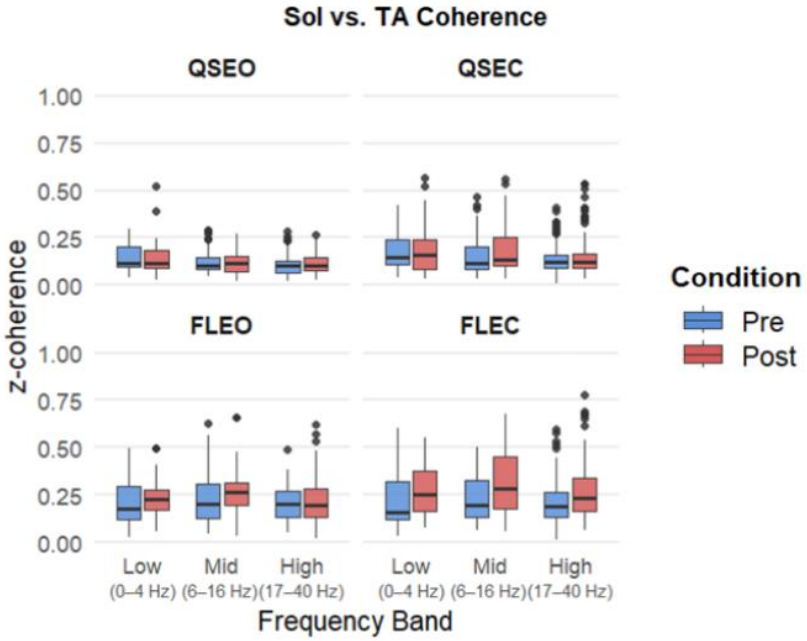


Figure 8: Boxplots of SOL–TA (agonist–antagonist) z-coherence by postural task (QSEO, QSEC, FLEO, FLEC) and frequency band [Low (0–4 Hz), Mid (6–16 Hz), High (17–40 Hz)], comparing Pre (blue) and Post (red) fatigue. Boxes show the interquartile range with median lines; whiskers indicate 1.5× IQR and points are outliers. Asterisks mark Bonferroni-adjusted Pre–Post differences within each task across the three bands (p < .05 = *, p < .01 = **).

Table 10: Results of the three-way repeated-measures ANOVAs examining the effects of fatigue, postural task, and frequency band on Fisher z-transformed GM-TA coherence for both eyes-open and eyes-closed conditions. Degrees of freedom and p values are Greenhouse–Geisser–adjusted where applicable; generalized eta squared (GES) is reported as the effect-size metric. Mean squared error (MSE) terms are reported per effect in the table. Sample size after exclusions due to missing data; n = 13 (df for the Condition main effect = 1,12).

| Effects | Eyes-open (AG-ANT) GM-TA | | | | | Eyes-closed (AG-ANT) GM-TA | | | | |
|---|---|---|---|---|---|---|---|---|---|---|
| | df(GG) | MSE | F | p-value | ges | df(GG) | MSE | F | p-value | ges |
| *Fatigue* | 1, 10 | 0.02 | 23.97*** | **<.001*** ** | 0.287 | 1, 11 | 0.03 | 7.21* | **0.021*** | 0.093 |
| *Postural Task* | 1, 10 | 0 | 3.93+ | 0.076 | 0.02 | 1, 11 | 0.01 | 3.16 | 0.103 | 0.014 |
| *Frequency Band* | 1.44, 14.39 | 0.01 | 2.45 | 0.132 | 0.019 | 1.34, 14.70 | 0.01 | 3.95+ | 0.056 | 0.022 |
| *Fatigue ×Postural Task* | 1, 10 | 0.01 | 0.21 | 0.655 | 0.002 | 1, 11 | 0.01 | 0.76 | 0.4 | 0.003 |
| *Fatigue × Frequency Band* | 1.56, 15.56 | 0 | 0.48 | 0.581 | 0.001 | 1.83, 20.12 | 0 | 0.21 | 0.797 | <.001 |
| *Postural Task × Frequency Band* | 1.72, 17.21 | 0 | 0.68 | 0.497 | 0.002 | 1.46, 16.07 | 0 | 2.62 | 0.115 | 0.006 |
| *Fatigue × Postural Task × Frequency Band* | 1.52, 15.25 | 0 | 2.25 | 0.147 | 0.009 | 1.24, 13.61 | 0 | 2.05 | 0.174 | 0.002 |

** p < .05; **p < .01; ***p < .001*

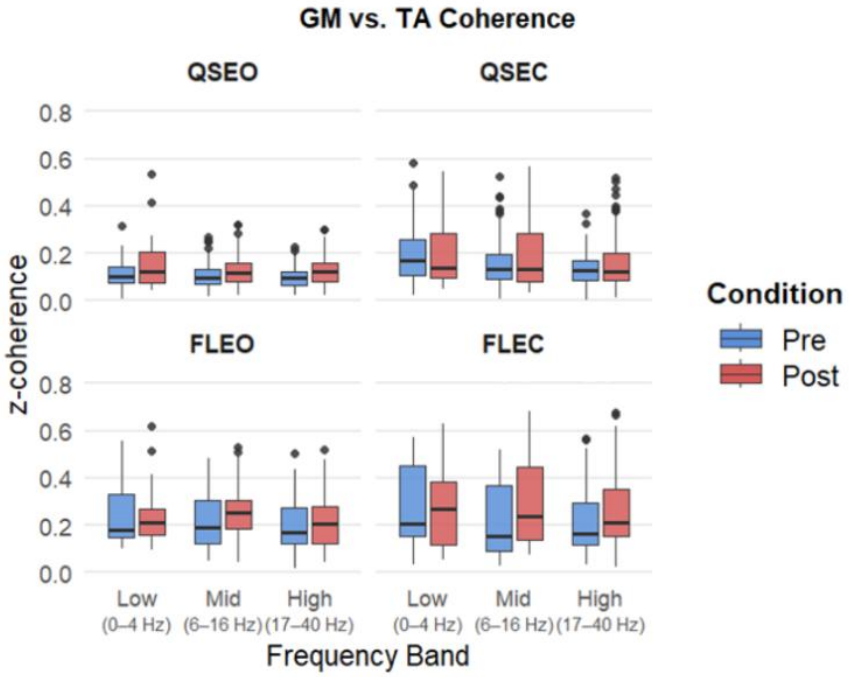


Figure 9: Boxplots of SOL–GM (agonist–agonist) z-coherence by postural task (QSEO, QSEC, FLEO, FLEC) and frequency band [Low (0–4 Hz), Mid (6–16 Hz), High (17–40 Hz)], comparing Pre (blue) and Post (red) fatigue. Boxes show the interquartile range with median lines; whiskers indicate 1.5× IQR and points are outliers. Asterisks mark Bonferroni-adjusted Pre–Post differences within each task across the three bands (p < .05 = *, p < .01 = **).

## 4.2. Center of Pressure (COP) metrics

### 4.2.1. SD, Velocity, and 95% Ellipse Area

Traditional stabilogram metrics revealed significant main effects of Postural Task and Vision for SD_ML. For all metrics, there was no significant fatigue or fatigue-related interaction effects. For SD_ML, Velocity, and EA95 there were significant main effects of Postural Task and Vision. For SD_AP, there was a main effect of Postural Task. A significant interaction effect was observed for EA95 of Postural Task x Vision (Table 11). In general, across the COP metrics, forward leaning caused higher values compared to quiet standing, whereas eyes-closed produced greater values than eyes-open

Table 11: Results of three way repeated-measures ANOVA examining the effects of Fatigue, Postural Task, and Vision on center-of-pressure (COP) measures of sway variability (SD_ML, SD_AP), sway velocity, and 95% confidence ellipse area (EA95). Significant main effects and interactions are highlighted in bold.

| Metric | Effect | df | MSE | F | p.value | GES | Metric | df | MSE | F | p.value | GES |
|---|---|---|---|---|---|---|---|---|---|---|---|---|
| *SD_ML* | Fatigue | 1, 13 | 0.01 | 0.92 | 0.354 | 0.003 | *SD_AP* | 1, 13 | 0.02 | 2.63 | 0.129 | 0.014 |
| | Postural Task | 1, 13 | 0.02 | 10.03 | **0.007** | 0.094 | | 1, 13 | 0.06 | 4.86 | **0.046** | 0.068 |
| | Vision | 1, 13 | 0.01 | 9.6 | **0.008** | 0.037 | | 1, 13 | 0.02 | 1.53 | 0.238 | 0.009 |
| | Fatigue* Postural Task | 1, 13 | 0.01 | 1.11 | 0.312 | 0.003 | | 1, 13 | 0.04 | 2.39 | 0.146 | 0.02 |
| | Fatigue*Vision | 1, 13 | 0.01 | 0.35 | 0.567 | 0.001 | | 1, 13 | 0.02 | 0.05 | 0.834 | <.001 |
| | Postural Task*Vision | 1, 13 | 0 | 4.1 | 0.064 | 0.006 | | 1, 13 | 0.02 | 2.17 | 0.165 | 0.011 |
| | Fatigue * Postural Task *Vision | 1, 13 | 0 | 0.02 | 0.887 | <.001 | | 1, 13 | 0.02 | 0.54 | 0.477 | 0.002 |
| *Velocity* | Fatigue | 1, 13 | 0.2 | 1.28 | 0.923 | <.001 | *EA95* | 1, 13 | 3.71 | 2.29 | 0.154 | 0.011 |
| | Postural Task | 1, 13 | 0.08 | 8.29 | **<.001** | 0.158 | | 1, 13 | 10.9 | 9.42 | **0.009** | 0.117 |
| | Vision | 1, 13 | 0.1 | 0.82 | **<.001** | 0.084 | | 1, 13 | 2.86 | 16.07 | **0.001** | 0.056 |
| | Fatigue* Postural Task | 1, 13 | 0.08 | 0.67 | 0.979 | <.001 | | 1, 13 | 3.08 | 0.64 | 0.437 | 0.003 |
| | Fatigue*Vision | 1, 13 | 0.05 | 2.78 | 0.896 | <.001 | | 1, 13 | 4.19 | 0.02 | 0.893 | <.001 |
| | Postural Task*Vision | 1, 13 | 0.07 | 1.29 | **0.003** | 0.036 | | 1, 13 | 2.56 | 4.76 | **0.048** | 0.015 |
| | Fatigue * Postural Task *Vision | 1, 13 | 0.07 | 9.15 | 0.902 | <.001 | | 1, 13 | 2.07 | 0.33 | 0.578 | <.001 |

** p < .05; **p < .01; ***p < .001*

### 4.2.2. Discrete Wavelet Transformation (DWT)

Figure 10 depicts the DWT (D1–D11) of a 30-s signal, illustrating scale-specific contributions across frequency bands. High-frequency details (D1–D4; ~3–50 Hz) show minimal amplitude, indicating little energy at rapid timescales. Mid-frequency bands (D5–D7; ~0.39–3.12 Hz) exhibit the most prominent, quasi-periodic fluctuations. Low-frequency components (D8–D11; ~0.02–0.39 Hz) are dominated by slow, large-amplitude oscillations and drift, reflecting long-timescale variations.

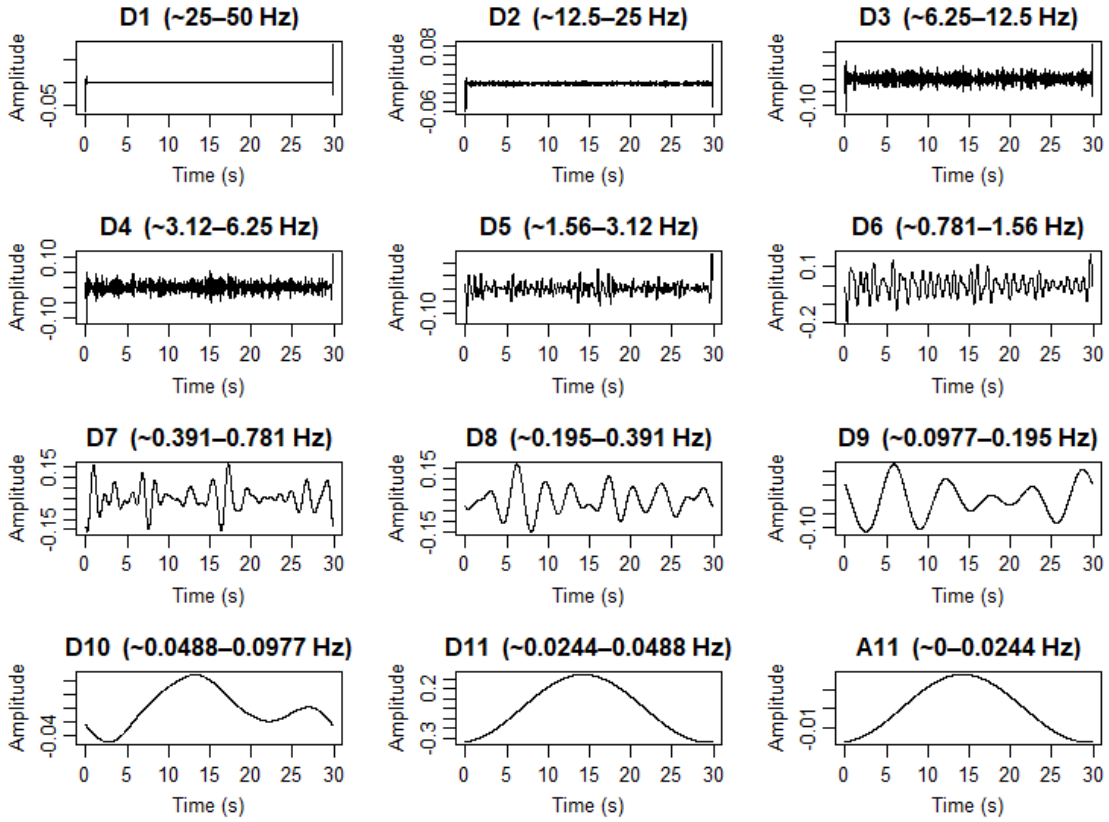


Figure 10: Maximal overlap discrete wavelet transform (MODWT; 'la8') of COP signal showing detail coefficients $D_1$–$D_{11}$ and the final approximation $A_{11}$over a 30-s trial.

Across both vision conditions (EO/EC) and axes (AP/ML), the DWT analyses showed a main effect of Frequency Band in every model (Tables 12 & 14). A main effect of Fatigue was not detected in any analysis, even though there were small changes in frequency bands following fatigue (Figures 10 & 11). For the AP axis, a significant Fatigue × Task × Band interaction was present for the EO condition. For the EC condition, a significant Postural Task main effect and a Fatigue × Task interaction were found. For the ML axis (Table 14), the EC condition exhibited a significant Postural Task main effect and a Task × Frequency band interaction (See Table A2 and Figures A4-5 in appendix for details concerning Task and Vision effects). The significant Fatigue-related interactions detected in specific models indicated that certain combinations of task and frequency band warranted further examination. Accordingly, post-hoc analyses were performed to identify which task–band pairings contributed to the observed interaction patterns.

A series of band-wise repeated-measures comparisons (Pre vs Post) were conducted for each task (QSEO, QSEC, FLEO, FLEC) on the anteroposterior (AP) wavelet bands (d1–d11; Table 13).

Generalized $\eta^2$ values for the fatigue term were uniformly small (typically ≤ .10, many < .01), and mean changes within bands were modest, indicating no fatigue effect that met the Bonferroni-adjusted threshold on either axis.

Table 12: Discrete Wavelet Transformation in anteroposterior plane repeated-measures ANOVA for Fatigue (Pre, Post), Postural Task (QS, FL), and Frequency Band. Entries: Greenhouse–Geisser df, MSE, F, p, generalized $\eta^2$ (GES).

| Effects | Discrete Wavelet Transformaiton EO-AP | | | | | Discrete Wavelet Transformaiton EC-AP | | | | |
|---|---|---|---|---|---|---|---|---|---|---|
| | df(GG) | MSE | F | p-value | ges | df(GG) | MSE | F | p-value | ges |
| Fatigue | 1, 13 | 0.17 | 0.2 | 0.659 | <.001 | 1, 13 | 0.1 | 0.38 | 0.548 | <.001 |
| Postural Task | 1, 13 | 0.23 | 0.66 | 0.43 | 0.002 | 1, 13 | 0.04 | 21.95 | **<.001*** ** | 0.012 |
| *Frequency Band* | 1.55, 20.20 | 2.08 | 144.54 *** | **<.001*** ** | 0.843 | 1.86, 24.17 | 0.8 | 251.16 | **<.001*** ** | 0.853 |
| Fatigue* Postural Task | 1, 13 | 0.12 | 0.65 | 0.434 | <.001 | 1, 13 | 0.03 | 10.38 | **0.007**** | 0.005 |
| *Fatigue × Frequency Band* | 1.89, 24.52 | 0.53 | 1.75 | 0.195 | 0.02 | 1.59, 20.62 | 0.53 | 0.84 | 0.422 | 0.011 |
| *Postural Task × Frequency Band* | 2.14, 27.85 | 0.55 | 2.96 + | 0.065 | 0.039 | 2.21, 28.68 | 0.67 | 3.14 | 0.054 | 0.067 |
| *Fatigue × Postural Task × Frequency Band* | 2.16, 28.12 | 0.2 | 5.64 ** | **0.008**** | 0.028 | 1.74, 22.65 | 0.43 | 1.62 | 0.221 | 0.019 |

** p < .05; **p < .01; ***p < .001*

Table 13: Discrete Wavelet Transformation (DWT) anteroposterior repeated-measures comparisons of Pre vs Post across tasks (QSEO, QSEC, FLEO, FLEC) for wavelet bands d1–d11 (frequency ranges indicated). Entries report F(df) for the Pre–Post factor, group means ± SE (Pre, Post), MSE, p, Bonferroni-corrected p, and generalized $\eta^2$ (GES).

| Anterior-Posterior | *Main effect - Fatigue* | | | | | | |
|---|---|---|---|---|---|---|---|
| | F(df) | Pre (Mean ± SE) | Post (Mean ± SE) | MSE | p | p (Bonferroni-corr.) | GES |
| **QSEO** | | | | | | | |
| *d1–d5 (1.56 - 50 Hz)* | 1.863 (1, 13) | 1.86 ± 0.30 | 3.07 ± 1.02 | 0.709 | 0.195 | 0.782 | 0.042 |
| *d6–d7 (0.39 - 1.56 Hz)* | 4.361 (1, 13) | 20.63 ± 3.48 | 12.78 ± 1.79 | 0.651 | 0.057 | 0.228 | 0.095 |
| *d8–d9 (0.09- 0.39 Hz)* | 6.030 (1, 13) | 30.58 ± 2.01 | 37.18 ± 3.27 | 0.247 | 0.029 | 0.116 | 0.076 |
| *d10–d11 (0.02 - 0.09 Hz)* | 0.150 (1, 13) | 48.82 ± 4.97 | 46.89 ± 4.49 | 0.649 | 0.705 | 1.000 | 0.002 |
| **QSEC** | | | | | | | |
| *d1–d5 (1.56 - 50 Hz)* | 0.524 (1, 13) | 2.15 ± 0.39 | 2.16 ± 0.27 | 0.363 | 0.482 | 1.000 | 0.014 |
| *d6–d7 (0.39 - 1.56 Hz)* | 0.003 (1, 13) | 24.32 ± 3.22 | 23.04 ± 1.74 | 0.350 | 0.958 | 1.000 | < 0.0001 |
| *d8–d9 (0.09- 0.39 Hz)* | 0.001 (1, 13) | 46.25 ± 2.20 | 46.53 ± 3.18 | 0.187 | 0.975 | 1.000 | < 0.0001 |
| *d10–d11 (0.02 - 0.09 Hz)* | 0.046 (1, 13) | 27.60 ± 2.95 | 28.27 ± 2.66 | 0.309 | 0.833 | 1.000 | 0.002 |
| ***FLEO*** | | | | | | | |
| *d1–d5 (1.56 - 50 Hz)* | 2.444 (1, 13) | 3.87 ± 1.09 | 2.32 ± 0.18 | 0.295 | 0.142 | 0.568 | 0.064 |
| *d6–d7 (0.39 - 1.56 Hz)* | 0.927 (1, 13) | 13.72 ± 2.81 | 10.84 ± 1.39 | 0.378 | 0.353 | 1.000 | 0.016 |
| *d8–d9 (0.09- 0.39 Hz)* | 0.464 (1, 13) | 33.39 ± 1.66 | 32.08 ± 2.77 | 0.162 | 0.508 | 1.000 | 0.011 |
| *d10–d11 (0.02 - 0.09 Hz)* | 3.757 (1, 13) | 49.00 ± 3.73 | 54.73 ± 2.57 | 0.271 | 0.075 | 0.298 | 0.062 |
| **FLEC** | | | | | | | |
| *d1–d5 (1.56 - 50 Hz)* | 5.324 (1, 13) | 4.88 ± 0.86 | 3.21 ± 0.55 | 0.440 | 0.038 | 0.153 | 0.090 |
| *d6–d7 (0.39 - 1.56 Hz)* | 4.431 (1, 13) | 27.51 ± 3.06 | 21.88 ± 1.78 | 0.292 | 0.055 | 0.221 | 0.064 |
| *d8–d9 (0.09- 0.39 Hz)* | 3.830 (1, 13) | 41.65 ± 3.20 | 47.76 ± 2.25 | 0.190 | 0.072 | 0.289 | 0.090 |
| *d10–d11 (0.02 - 0.09 Hz)* | 0.000 (1, 13) | 25.53 ± 2.26 | 26.37 ± 3.13 | 0.349 | 1.000 | 1.000 | < 0.0001 |

** p < .05; **p < .01; ***p < .001*

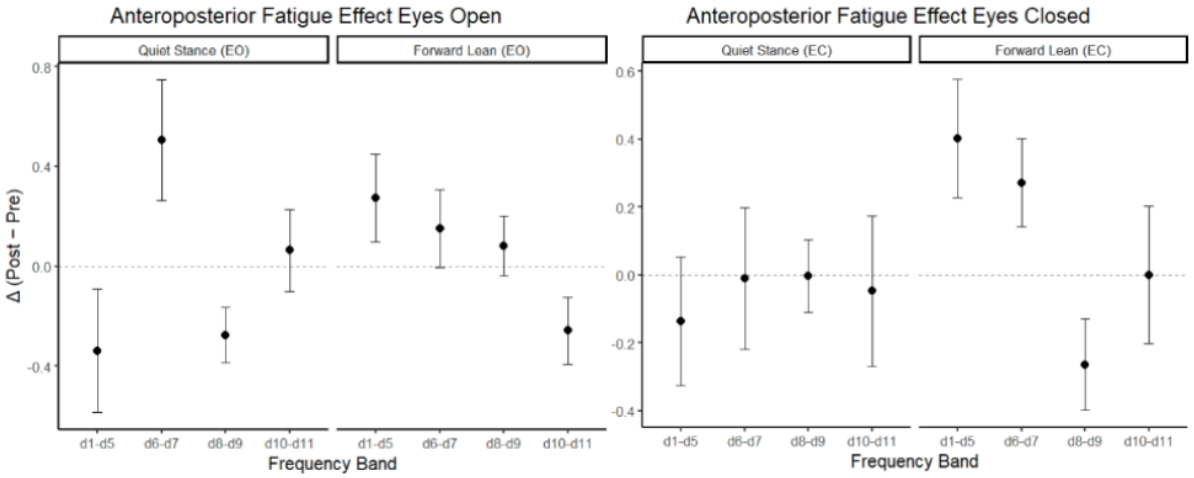


Figure 11: Anteroposterior fatigue-induced changes across frequency bands under EO and EC conditions. Mean (± SEM) differences (Δ = Post − Pre) are presented for QS and FL postural tasks. Data were logit-transformed using the function log(p / (1 − p)) to normalize proportional energy values constrained between 0 and 1. A more negative Δ denotes a stronger post-fatigue effect, reflected by an increased share of energy within that frequency band compared to pre-fatigue

Table 14: Discrete Wavelet Transformation in mediolateral plane repeated-measures ANOVA for Fatigue (Pre, Post), Postural Task (QS, FL), and Frequency Band. Entries: Greenhouse–Geisser df, MSE, F, p, generalized $\eta^2$ (GES).

| Effects | Discrete Wavelet Transformaiton EO-ML | | | | | Discrete Wavelet Transformaiton EC-ML | | | | |
|---|---|---|---|---|---|---|---|---|---|---|
| | df(GG) | MSE | F | p-value | ges | df(GG) | MSE | F | p-value | ges |
| Fatigue | 1, 13 | 0.08 | 0.06 | 0.816 | <.001 | 1, 13 | 0.13 | 0.31 | 0.59 | <.001 |
| Postural Task | 1, 13 | 0.04 | 0.01 | 0.905 | <.001 | 1, 13 | 0.1 | 6.49 | **0.024*** | 0.007 |
| *Frequency Band* | 1.88, 24.42 | 1.75 | 128.5 | **<.001*****| 0.838 | 1.51, 19.63 | 2.62 | 98.25 | **<.001***** | 0.808 |
| Fatigue* Postural Task | 1, 13 | 0.05 | 3.14 | 0.1 | 0.002 | 1, 13 | 0.13 | 0.2 | 0.665 | <.001 |
| *Fatigue × Frequency Band* | 1.61, 20.93 | 0.62 | 1.95 | 0.172 | 0.023 | 1.90, 24.73 | 0.43 | 0.88 | 0.424 | 0.008 |
| *Postural Task × Frequency Band* | 1.71, 22.24 | 0.33 | 1.12 | 0.337 | 0.008 | 1.96, 25.54 | 0.3 | 4.42 | **0.023*** | 0.027 |
| *Fatigue × Postural Task × Frequency Band* | 1.44, 18.72 | 0.58 | 0.71 | 0.461 | 0.007 | 2.29, 29.73 | 0.4 | 1.9 | 0.163 | 0.018 |

** p < .05; **p < .01; ***p < .001*

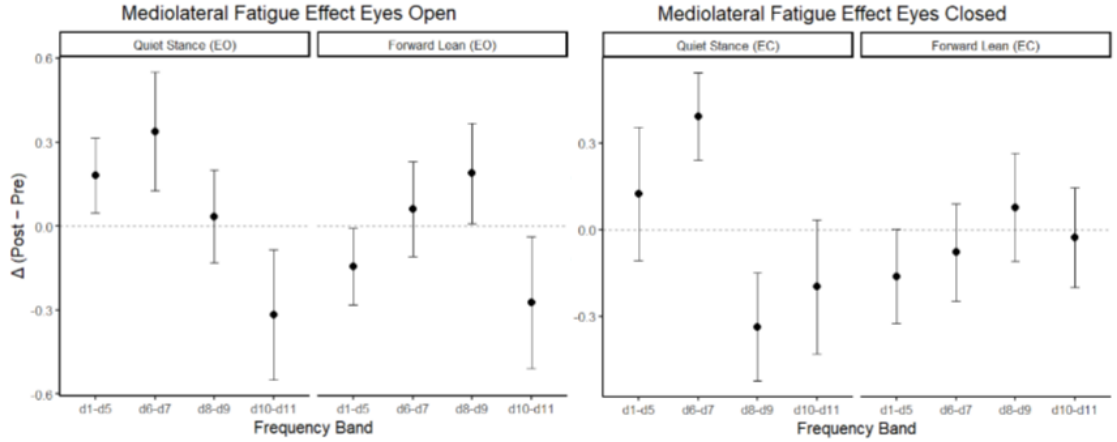


Figure 12: Mediolateral fatigue-induced changes across frequency bands under EO and EC conditions. Mean (± SEM) differences (Δ = Post − Pre) are presented for QS and FL postural tasks. Data were logit-transformed using the function log(p / (1 − p)) to normalize proportional energy values constrained between 0 and 1. A more negative Δ denotes a stronger post-fatigue effect, reflected by an increased share of energy within that frequency band compared to pre-fatigue.

### 4.3. Pearson Correlations

Correlations between the pre–post changes in the three coherence pairs (Δ SOL – GM, Δ SOL – TA, Δ GM – TA) and DWT bands were examined by task (Tables 15 – 17). For the AG – AG pair, there was a significant correlation in QS for EO between the high frequency coherence band and the open-loop DWT band ($p = 0.025$). Otherwise, correlations were weak in magnitude and did not reach statistical significance ($p > .05$).

Table 15: Pearson correlation coefficients (r) and p-values between AG–AG coherence bands and relative energy in DWT bands for the Δ (post–pre) comparison.

| Δ AG-AG Coherence bands | Task | Open Loop | | Somatosensory | | Vestibular | | Visual | |
|---|---|---|---|---|---|---|---|---|---|
| | | r | p | r | p | r | p | r | p |
| *Low (0-3.94 Hz)* | QSEO | -0.326 | 0.278 | 0.179 | 0.559 | 0.458 | 0.116 | -0.3 | 0.319 |
| *Mid (5.92-15.78 Hz)* | QSEO | -0.44 | 0.132 | -0.074 | 0.81 | 0.466 | 0.108 | 0.044 | 0.887 |
| *High (17.75-39.45 Hz)* | QSEO | -0.616 | **0.025** | -0.359 | 0.228 | 0.284 | 0.346 | 0.399 | 0.177 |
| *Low (0-3.94 Hz)* | QSEC | 0.464 | 0.095 | 0.273 | 0.345 | -0.065 | 0.826 | -0.248 | 0.392 |
| *Mid (5.92-15.78 Hz)* | QSEC | 0.448 | 0.108 | 0.265 | 0.36 | -0.34 | 0.234 | -0.086 | 0.77 |
| *High (17.75-39.45 Hz)* | QSEC | 0.531 | 0.051 | 0.363 | 0.202 | -0.412 | 0.143 | -0.116 | 0.692 |
| *Low (0-3.94 Hz)* | FLEO | -0.127 | 0.666 | -0.024 | 0.935 | 0.146 | 0.618 | -0.058 | 0.844 |
| *Mid (5.92-15.78 Hz)* | FLEO | -0.101 | 0.732 | 0.271 | 0.348 | -0.405 | 0.151 | 0.17 | 0.561 |
| *High (17.75-39.45 Hz)* | FLEO | 0.045 | 0.878 | 0.198 | 0.498 | -0.052 | 0.859 | -0.113 | 0.699 |
| *Low (0-3.94 Hz)* | FLEC | 0.105 | 0.721 | -0.046 | 0.877 | -0.021 | 0.942 | -0.042 | 0.886 |
| *Mid (5.92-15.78 Hz)* | FLEC | 0.152 | 0.603 | 0.064 | 0.828 | -0.181 | 0.536 | 0.033 | 0.912 |
| *High (17.75-39.45 Hz)* | FLEC | 0.048 | 0.871 | -0.227 | 0.435 | -0.346 | 0.226 | 0.416 | 0.139 |

** p < .05; **p < .01; ***p < .001*

Table 16: Pearson correlation coefficients (r) and p-values between AG–ANT (Sol – TA) coherence bands and relative energy in DWT bands for a Δ (post – pre) comparison.

| Δ AG-ANT (SOL-TA) Coherence bands | Task | Open loop | | Somatosensory | | Vestibular | | Visual | |
|---|---|---|---|---|---|---|---|---|---|
| | | r | p | r | p | r | p | r | p |
| *Low (0-3.94 Hz)* | QSEO | 0.139 | 0.6832 | 0.209 | 0.5379 | 0.339 | 0.3081 | 0.122 | 0.7209 |
| *Mid (5.92-15.78 Hz)* | QSEO | 0.093 | 0.7866 | 0.101 | 0.7686 | -0.073 | 0.8314 | 0.326 | 0.3285 |
| *High (17.75-39.45 Hz)* | QSEO | 0.135 | 0.6924 | 0.141 | 0.6797 | 0.082 | 0.8113 | 0.23 | 0.4971 |
| *Low (0-3.94 Hz)* | QSEC | -0.209 | 0.5138 | -0.202 | 0.528 | 0.073 | 0.8225 | 0.164 | 0.6095 |
| *Mid (5.92-15.78 Hz)* | QSEC | -0.405 | 0.1918 | -0.392 | 0.208 | 0.052 | 0.8719 | 0.376 | 0.2289 |
| *High (17.75-39.45 Hz)* | QSEC | -0.232 | 0.4691 | -0.364 | 0.2453 | -0.218 | 0.496 | 0.448 | 0.1445 |
| *Low (0-3.94 Hz)* | FLEO | 0.116 | 0.7198 | 0.2 | 0.5329 | -0.217 | 0.4986 | -0.026 | 0.9366 |
| *Mid (5.92-15.78 Hz)* | FLEO | 0.169 | 0.5986 | 0.014 | 0.9663 | -0.282 | 0.3741 | 0.148 | 0.6463 |
| *High (17.75-39.45 Hz)* | FLEO | -0.069 | 0.8302 | -0.261 | 0.4133 | -0.002 | 0.9954 | 0.225 | 0.4829 |
| *Low (0-3.94 Hz)* | FLEC | -0.335 | 0.2868 | 0.001 | 0.9966 | 0.114 | 0.7236 | -0.089 | 0.7826 |
| *Mid (5.92-15.78 Hz)* | FLEC | -0.068 | 0.834 | 0.09 | 0.7804 | -0.155 | 0.6307 | 0.062 | 0.8488 |
| *High (17.75-39.45 Hz)* | FLEC | 0.108 | 0.7372 | 0.095 | 0.7698 | -0.078 | 0.8094 | -0.066 | 0.8378 |

Table 17: Pearson correlation coefficients (r) and p-values between AG–ANT (GM – TA) coherence bands and relative energy in DWT bands for a Δ (post – pre) comparison.

| **Δ AG-ANT (GM-TA) Coherence bands** | **Task** | **Open loop** | | **Somatosensory** | | **Vestibular** | | **Visual** | |
|---|---|---|---|---|---|---|---|---|---|
| | | **r** | **p** | **r** | **p** | **r** | **p** | **r** | **p** |
| *Low (0-3.94 Hz)* | QSEO | 0.123 | 0.7181 | 0.108 | 0.7518 | 0.4 | 0.2225 | 0.181 | 0.5952 |
| *Mid (5.92-15.78 Hz)* | QSEO | 0.189 | 0.5787 | 0.128 | 0.7075 | -0.085 | 0.8047 | 0.3 | 0.3698 |
| *High (17.75-39.45 Hz)* | QSEO | 0.422 | 0.1957 | -0.12 | 0.7253 | -0.31 | 0.3529 | 0.259 | 0.4423 |
| *Low (0-3.94 Hz)* | QSEC | -0.134 | 0.6774 | -0.152 | 0.6372 | -0.039 | 0.9038 | 0.164 | 0.6107 |
| *Mid (5.92-15.78 Hz)* | QSEC | -0.079 | 0.8079 | -0.174 | 0.589 | -0.209 | 0.5154 | 0.246 | 0.4407 |
| *High (17.75-39.45 Hz)* | QSEC | -0.135 | 0.6749 | -0.296 | 0.3497 | -0.3 | 0.3432 | 0.401 | 0.196 |
| *Low (0-3.94 Hz)* | FLEO | 0.124 | 0.7009 | 0.212 | 0.5092 | -0.28 | 0.3778 | 0.012 | 0.9704 |
| *Mid (5.92-15.78 Hz)* | FLEO | -0.027 | 0.934 | -0.132 | 0.6832 | -0.377 | 0.2271 | 0.403 | 0.1945 |
| *High (17.75-39.45 Hz)* | FLEO | 0.016 | 0.9605 | -0.23 | 0.4719 | -0.22 | 0.4925 | 0.339 | 0.2807 |
| *Low (0-3.94 Hz)* | FLEC | -0.448 | 0.1441 | -0.129 | 0.6899 | 0.284 | 0.3712 | -0.083 | 0.797 |
| *Mid (5.92-15.78 Hz)* | FLEC | -0.362 | 0.247 | -0.322 | 0.3074 | -0.088 | 0.7855 | 0.29 | 0.3608 |
| *High (17.75-39.45 Hz)* | FLEC | -0.125 | 0.6987 | -0.23 | 0.4728 | -0.177 | 0.583 | 0.279 | 0.3794 |

# Chapter 5: Discussion

The main results of this thesis revealed that fatigue effects were primarily manifested through enhanced intermuscular coordination rather than global postural changes. The co-contraction index (CCI) showed no significant fatigue effects and was driven by task demands rather than fatigue. Intermuscular coherence demonstrated task-dependent adaptations, with agonist-agonist (SOL-GM) coherence increasing significantly in mid- and high-frequency bands (6-40 Hz) only during the most challenging condition (forward lean, eyes-closed, $p < 0.01$), while AG–ANT coherence increased generally across all bands. For velocity, changes were small and context dependent, with a decrease observed only in FLEO and no measurable differences in the other task-vision combinations. In general, traditional COP variables did not change post fatigue. The DWT analysis revealed only small fatigue-induced changes in frequency band energy distributions, with energy remaining concentrated in closed-loop frequencies (<1 Hz). Pearson correlations between coherence changes and DWT-derived sensory bands were largely non-significant ($p > 0.05$).

## 5.1. EMG Amplitude and Co-contraction

In this study, we examined how NMF influences neuromuscular and postural stability mechanisms in two postural tasks. To examine neuromuscular alterations post-fatigue, we examined the activation, CCI, and coherence between agonist and antagonist muscle groups. We hypothesized an increase in EMG amplitudes following fatigue. However, no significant amplitude changes were observed for SO and TA, whereas the GM exhibited a slight post-fatigue decrease in activation during the postural trials, which was significant only for the FLEO condition. This pattern could be associated with a motor reweighting strategy, in which the central nervous system transiently down-weights a fatigued, less reliable plantarflexor and relies on other muscles (ankle or more proximal joints) to maintain balance[15,115,116]. The level of co-contraction was determined primarily by the postural task, with minimal influence of fatigue. These findings refute our hypothesis of increased co-contraction following fatigue, but are in line with the results of Jo and Bilodeau[91]. Therefore, an increase in active ankle stiffness through increased co-activation of GM or SO and TA to compensate for the effects of fatigue does not appear to be at play in our study. CCI appeared to be modulated by the postural task, with higher values typically observed under

conditions requiring increased joint stiffness or co-contraction to preserve stability, particularly in the task of greater complexity, the FL task. This modulation suggests that AG – ANT interactions are not static but dynamically adjusted in response to task demands, sensory availability, and perturbation characteristics[6,117,118]. Visual state also appeared to slightly influence co-contraction, with higher (but not significant) CCI observed during EC conditions relative to EO. This aligns with prior evidence that visual deprivation leads to increased muscle co-activation and joint stiffness as a compensatory mechanism to maintain postural stability[6,119,120]. Together, these findings indicate that both task complexity (FL versus QS) and sensory context (EO versus EC) shaped neuromuscular strategies for postural control, whereas the effect of fatigue was negligible.

### 5.2. Coherence

Increases in AG-AG coherence typically indicate common synaptic (neural) input to synergistic motor pools and thus stronger functional coupling within a muscle synergy[114]. AG–ANT pairs show increased intermuscular coherence, in the high frequency range (16 – 30 Hz), which may reflect shared drive during simultaneous activation[38]. In addition to reports emphasizing task-related modulation primarily in AG–AG coherence[45,121], we observed task- and fatigue-dependent changes that were also present in AG–ANT pairs (Figures 8 and 9). This aligns with evidence that intermuscular coherence is modulated by task demands across both synergistic and opposing muscle pairs, including the ankle flexor–extensor system[45,50,114,122]. Thus a shift towards increased intermuscular coordination to preserve stability under heightened postural demands[46]. In the present study, as postural task demands increased under fatigue, higher coherence values were observed for both agonists and antagonists muscle pairs, suggesting a greater requirement for coordinated activation between muscles to counteract increased postural task demands under fatigue. This elevated coherence is often interpreted as reflecting increased cortical and subcortical drive to stabilize posture during demanding conditions[45].

The CNS typically up-scales common synaptic drive to synergistic and antagonist muscles, which manifests as stronger intermuscular EMG–EMG coherence across frequency bands. Empirical studies show fatigue-related increases in intermuscular (especially high-band) coherence[50,103,105,123]. We hypothesized that fatigue would increase coherence in all frequency

bands and that these effects would depend on task demands with increases being more pronounced in the forward leaning task. Overall, our findings partially support this hypothesis. Coherence showed a general increase in both AG‑ANT muscle pairs with fatigue, indicating enhanced coupling of subcortical and corticospinal levels[45]. The increase in AG–ANT coherence following fatigue indicates enhanced neuromuscular coupling and synchronization of common neural drive to agonist and antagonist muscle pairs during postural control. This elevated coherence reflects increased corticospinal and subcortical synchronization, which may serve as a compensatory mechanism to preserve joint stability when proprioceptive feedback is degraded by fatigue[24,44–46]. Furthermore, significant fatigue effects in mid and high-band range were observed for the AG–AG pair in the FLEC condition, consistent with increased corticospinal synchronization. Thus, fatigue appears to engage in compensatory mechanisms, wherein corticospinal feedback maintains local stability and coordinates global muscle activity to preserve balance[104]. These compensations likely reflect increased reliance on shared neural input and greater synchronization among synergistic muscles, representing adaptations that stabilize the fatigued joint despite reduced individual muscle capacity[15,114]. These adaptations support the idea that both synergistic AG–AG and reciprocal AG–ANT muscle pairs coordinate to preserve stability in the presence of NMF[124]. The most challenging balance task (FLEC) presented with fatigue-related increases in coherence in the mid to high frequency ranges (5–16Hz and 16- 40 Hz) reflecting enhanced corticospinal drive and compensatory cortical recruitment involvement in AG–AG[44,114,122], whereas the easier quiet standing tasks showed no change. This suggests that postural demands of a simple quiet stance are not enough for the impacts of NMF to cause significant alterations into coherence patterns. This interpretation aligns with previous work showing that quiet standing is largely regulated by subcortical circuits (0 – 4 Hz), with minimal corticospinal engagement[51,125,126]. The task-dependent modulation of coherence, with increases observed primarily during the most challenging condition (FLEC) rather than during simpler quiet standing, suggests that neuromuscular coupling strategies are dynamically adjusted based on ongoing task demands and are primarily reflective of a feedback reactive response[24]. Taken together, these results support the view that fatigue influences postural control primarily when task demands exceed the stabilizing capacity of subcortical mechanisms, thereby necessitating additional corticospinal involvement to maintain balance.

The apparent inconsistency between increased AG‑ANT coherence and unchanged CCI following fatigue can be reconciled by recognizing that these two measures capture different aspects of neuromuscular coordination. CCI quantifies the amplitude of simultaneous muscle activation (e.g., the degree of overlapping EMG activity in the time domain)[24,127,128]. In contrast, coherence measures the temporal synchronization and frequency-domain correlation of common neural drive to motor pools, reflecting shared oscillatory inputs from cortical and subcortical sources that do not necessarily alter the absolute amplitude of muscle activation[24]. A few factors in the data make this explanation plausible. First, fatigue did not elevate overall EMG amplitudes, and the GM showed a post-fatigue decrease, which would blunt or offset any increase in amplitude overlap captured by CCI, even as central coupling strengthened (increased AG–ANT coherence). Second, coherence increases were band- and task-specific (notably in mid/high bands during FLEC), reflecting enhanced corticospinal/subcortical synchronization under higher demand, whereas CCI would be insensitive to brief, frequency-specific co-activation that does not increase mean overlap.

### 5.3. COP Traditional Metrics

Overall, there were no major changes in standard COP metrics, including 95% ellipse area, mean velocity, or the standard deviations of ML and AP sway. Although we initially expected an increase in sway velocity based on prior research[9,86,87,90,91], the present pattern aligns with studies showing that visual feedback, such as maintaining eye fixation on a stationary target, can reduce postural sway following calf fatigue[93,94]. This selective reduction is most plausibly interpreted as a visually supported tightening of postural control, reflecting a cautious stiffening strategy and increased external attentional focus when the COM is anteriorly displaced and visual information can be exploited for precise error correction[75,77,129]. Consistent with this interpretation, we observed a modest decrease in GM activation in the same FLEO condition, which is compatible with heightened reliance on visual cues and coincides with the notion of an external attentional focus[130]. Context dependence is consistent with reports that fatigue can either increase or decrease sway depending on task and sensory constraints, including observations of reduced COP excursions after targeted muscle fatigue and meta-analytic evidence that fatigue effects vary with experimental conditions[95,131]. Previous studies have reported reductions in total COP path length and mean COP

velocity during single-leg stance with eyes open following exercise, indicating diminished sway and slower COP excursions[95]. When the ankle musculature is fatigued, mean COP velocity has been shown to remain unchanged, whereas fatigue of muscles acting at the knee or hip leads to increases in COP velocity during single-leg, eyes-open stance[70]. The absence of broader changes across COP parameters is consistent with previous research showing that NMF often induces subtle or task-specific rather than global alterations in postural stability, with several studies reporting no significant changes in sway area, amplitude, or mean velocity following fatigue during different postural task[17,95,132,133]. However, see the limitations section below.

### 5.4. Discrete Wavelet Transformation

In both the AP and ML directions, the COP displacements were decomposed into different frequency intervals to characterize open-loop (>1 Hz) and closed-loop (<1 Hz) processes of postural control. Even though significant fatigue interactions were found for the AP direction, none of the post hoc tests showed significant pre-to-post fatigue changes in frequency band energy. No fatigue main effect or interactions were found for the ML plane, contrary to our hypothesis. These results are broadly consistent with an earlier study that used Discrete Fourier Transform–based power spectrum analysis across frequency bands (0–0.3, 0.3–1, and 1–3 Hz)[91]. Notably, this study reported generally no fatigue effect except for a small increase in ML COP power confined to the 1–3 Hz band[91]. Other investigations using DWT have detected distinct frequency-dependent fatigue signatures: reduced proprioceptive band energy (1.56-6.25 Hz) under mental fatigue conditions[98] and selective ultralow (<0.10 Hz) and moderate (1.56-6.25 Hz) band modulation with neck muscle fatigue[20], demonstrating that wavelet decomposition can reveal frequency-specific adaptations masked by traditional aggregate COP metrics[20,98]. The discrepancy between our null findings and these positive results may stem from several factors. First, fatigue type matters: localized plantar flexor fatigue may produce different frequency-specific COP adaptations compared to mental fatigue (which affects central processing) or neck muscle fatigue (which compromises head stabilization and vestibular signalling. Second, it is possible that our relatively short fatigue protocol (see Limitations) may have induced insufficient perturbation to the postural control system to manifest as detectable frequency-band energy shifts. Third, the specific

frequency band definitions and wavelet parameters used across studies vary, and our particular decomposition scheme may not have optimally captured the frequency ranges most sensitive to plantar flexor fatigue[134].

Synthesizing the coherence and DWT findings, the results indicate that fatigue-related alterations are frequency and plane specific rather than global and thus may not appear uniformly across conditions. While DWT-derived COP band energies showed no systematic pre to post changes, agonist-agonist intermuscular coherence increased under higher task demand, suggesting that these adaptations occurred chiefly at corticospinal and subcortical levels, reflecting enhanced synchronization of common neural drive rather than overt changes in mechanical sway. Thus, the prevailing adjustment is characterized less by changes in peripheral output (e.g., sway amplitude or velocity) and more by central coordination mechanisms, consistent with evidence that fatigue can strengthen shared neural input without altering traditional COP metrics[135].

The closed-loop region reflects long-term regulatory system contributions, where sensory feedback (visual, vestibular, and proprioceptive) is integrated to postural reactions. This region showed the largest sway energy contributions across all conditions, consistent with the dominant role of feedback in postural stability. Furthermore, the eyes-closed condition is associated with lower energy contributions in the highest band (d10–d11) across both QS and FL in both pre and post blocks, relative to eyes-open (see Appendix). This pattern aligns with sensory reweighting and the expected reduction in visually mediated feedback when vision is removed[13,14]. In both AP and ML directions, the open-loop region exhibited low energy contributions relative to closed-loop levels, consistent with evidence that short-latency sway is less influential in sustained balance control[21,72,113,136]. While these mechanisms provide short-term stability, they are metabolically costly and less adaptable, promoting an overall need to utilize a closed-loop sensory system for postural control efficiency[21,137]. This organization is consistent with established descriptions during quiet-stance sway, which report dominant energy contributions below ~1 Hz and emphasize that COP measures primarily reflect long latency sensory feedback corrections[72,113,136,138].

Consistent with the sensory-reweighting theory, the postural control system adjusts the relative reliance on available inputs as task and environmental constraints change. When visual information is removed, energy in the band linked to visually mediated feedback (d10–d11) declines, with a concomitant increase in the bands commonly associated with proprioceptive and

vestibular contributions (d6–d7, d8–d9)[55,61,67]. This pattern indicates a shift toward greater weighting of non-visual cues to maintain stability. In the present study, we found no change in the redistribution of energy due to fatigue, whereas previous studies have shown an increased reliance on the vestibular or visual sensory systems when proprioceptive signals are degraded due to fatigue[16,94,139]. Though the changes were not significant, both the anteroposterior and mediolateral axes showed fatigue-related modifications. Across axes, there was a modest, non-significant decrease in the putative proprioceptive band (d6–d7) after fatigue under both eyes-open and eyes-closed conditions, except for the FLEC task in the mediolateral axis. This pattern is consistent with sensory reweighting: when somatosensory reliability is reduced by fatigue, the nervous system increases reliance on vestibular and, when available, visual inputs to generate the joint torque and stiffness required to stabilize the body during forward-lean demands[61]. Mechanically, as the COM moves anteriorly, passive ankle stiffness contributes less to restoring torques, necessitating greater active regulation by the plantarflexors in the anteroposterior direction; simultaneously, the reduced mediolateral margin of stability increases the need for precise ankle torque modulation to constrain COM motion in the frontal plane[3,61].

### 5.5. Pearson correlation

Correlation analyses focused on the association between fatigue-related changes in coherence frequency bands versus those in DWT bands (however, correlation analyses between raw coherence and DWT values are presented in appendix for both pre- and post-fatigue). Contrary to our hypothesis, across all tests, correlations remained nonsignificant, indicating no consistent linear relationship between changes in coherence (Δ) and those in DWT-derived sensory bands (open loop, somatosensory, vestibular, visual). The only exception was a significant negative association observed in the QSEO condition between the high frequency AG-AG coherence band and the open-loop DWT band. Within stabilogram-diffusion analysis (rambling and trembling, SDA, DFA) the open-loop (short-term) regime reflects sway before corrective feedback is re-engaged. Importantly, several studies interpret this portion of quiet-stance sway as exploratory behavior, characterized by small, purposeful fluctuations that actively probe the environment to enhance both postural stability and perceptual recalibration[140,141]. Evidence shows that sway

characteristics in the open-loop window connect with visual conditions and can facilitate task performance, consistent with an exploratory role[21]. This interpretation suggests that, rather than being purely noise, open-loop fluctuations may serve as an adaptive mechanism by which the CNS continuously updates its internal model of balance control. However, this interpretation should be considered cautiously given our findings. The absence of consistent effects across planes (ML showed no fatigue effects) and task-specificity limited to the most challenging condition suggest these patterns could represent random variation or spurious findings rather than robust, generalizable neuromuscular responses to fatigue[142].

This study demonstrates that task context exerts a clear influence on neuromuscular coordination, with forward leaning eliciting distinct adjustments. Our findings that fatigue effects are context-dependent rather than universally destabilizing represent an advancement in understanding postural control, reframing fatigue not as a simple deficit but as part of a complex, adaptive system that responds to task demands. Collectively, these findings suggest that the effects of fatigue are relatively subtle compared with the dominant influence of task demands and sensory context. This reframes fatigue not as a direct destabilizer but as a context-dependent modulator of postural control that interacts with visual and proprioceptive signals to maintain equilibrium. The absence of major changes in mechanical sway metrics, coupled with neural-level adaptations evident in coherence, supports the notion that the central nervous system reorganizes control strategies rather than simply degrading performance under fatigue. From a clinical perspective, these results emphasize that rehabilitation and balance training aimed at enhancing fatigue resilience should incorporate task-specific and sensory-based paradigms, for example by manipulating visual feedback or stance configuration, to better reveal, challenge, and strengthen compensatory control mechanisms in populations with reduced postural robustness.

### 5.6. Limitations

This study highlights the fact that fatigue effects are context-dependent rather than universally destabilizing and should be considered in the context of a complex, adaptive system that responds to task demands. Several limitations do warrant consideration and are discussed here. First, both coherence analysis and DWT analysis can be sensitive to methodological parameters (coherence:

window length, normalization, EMG preprocessing; DWT: choices of mother wavelet, filter length, boundary handling, and decomposition levels), which could influence associated physiological interpretations. Our fatigue protocol may not have induced sufficiently robust effects in the present sample of participants, as evidenced by the lack of change in traditional COP metrics and shorter fatigue task durations compared with a recent similar study[18]. This could explain the absence of post-hoc differences despite significant interactions found in the ANOVAs. Also, our conservative approach for the Bonferroni correction for multiple comparisons may have reduced power to detect genuine but subtle fatigue effects. Our sample size calculation was based on changes in one coherence frequency band (alpha) with fatigue. However, we decided to also include the factor 'frequency bands' (Bands) in our ANOVA models, thus an additional factor, which may have resulted in an underpowered study for the number of subjects recruited. However, it should be noted that fatigue effects and fatigue-related interaction were indeed observed for EMG coherence. Furthermore, coherence analysis captures only linear associations between pairs of signals; however, neuromuscular coordination during postural control often exhibits both linear and non-linear characteristics, reflecting complex interactions across multiple neural and mechanical subsystems[143]. Finally, the task-specific nature of fatigue limits generalizability, as different fatigue protocols or muscle groups may yield different postural control adaptations.

## Chapter 6: Conclusion, Implications, and Future Directions

This thesis investigated the effects of NMF on postural control, assessed through muscle activation strategies (EMG) and analysis of COP movements, in healthy young adults, providing important insights into the neuromuscular adaptations that occur when the postural control system is challenged by both fatigue and task complexity. The findings demonstrate that fatigue effects on postural control are subtle and highly task-dependent. Rather than producing global instability, localized ankle muscle fatigue primarily resulted in enhanced intermuscular coordination strategies, particularly increased AG‑AG corticospinal drive evidenced by higher-frequency coherence in challenging postural conditions and a general increase in AG‑ANT coherence reflecting enhanced neuromuscular coupling between agonist and antagonist muscle pairs. The results suggest that standard clinical balance assessments performed under simple conditions may fail to detect fatigue-related deficits that become apparent under more challenging circumstances. Rehabilitation protocols should therefore incorporate progressively challenging postural tasks and consider both sensory (visual state) and task contexts to reveal underlying deficits and optimize intervention strategies. Future research directions should explore how these fatigue-related adaptations manifest in diverse postural task and different clinical populations. Additionally, longitudinal studies examining the temporal dynamics of coherence modulation during the transition from pre-task anticipatory phases to ongoing postural control would help distinguish between proactive (feedforward) and reactive (feedback-driven) compensatory mechanisms. In conclusion, this research advances our understanding of the complex interactions between muscle fatigue, sensory integration, and postural control, demonstrating that the nervous system's adaptive capacity extends well beyond simple compensatory muscle activation to include sophisticated neural coordination strategies that preserve stability under challenging conditions.

## References


1. Shumway-Cook, A. & Woollacott, M. H. Motor Control: Translating Research into Clinical Practice. (Wolters Kluwer, 2017).
2. Lafond, D., Duarte, M. & Prince, F. Comparison of three methods to estimate the center of mass during balance assessment. *J. Biomech.* **37**, 1421–1426 (2004).
3. Winter, D. Human balance and posture control during standing and walking. *Gait Posture* **3**, 193–214 (1995).
4. Masani, K., Popovic, M. R., Nakazawa, K., Kouzaki, M. & Nozaki, D. Importance of body sway velocity information in controlling ankle extensor activities during quiet stance. *J. Neurophysiol.* **90**, 3774–3782 (2003).
5. Watanabe, T., Saito, K., Ishida, K., Tanabe, S. & Nojima, I. Age-Related Declines in the Ability to Modulate Common Input to Bilateral and Unilateral Plantar Flexors During Forward Postural Lean. *Front. Hum. Neurosci.* **12**, (2018).
6. Fok, K. L. *et al.* Co-contraction of ankle muscle activity during quiet standing in individuals with incomplete spinal cord injury is associated with postural instability. *Sci. Rep.* **11**, 19599 (2021).
7. Hurd, W. J. & Snyder-Mackler, L. Neuromuscular Training. in *Orthopaedic Rehabilitation of the Athlete: Getting Back in the Game* 247–260 (Elsevier, Philadelphia, 2007). doi:10.1016/B978-044306642-9.50018-6.
8. Monjo, F. & Forestier, N. Unexperienced mechanical effects of muscular fatigue can be predicted by the Central Nervous System as revealed by anticipatory postural adjustments. *Exp. Brain Res.* **232**, 2931–2943 (2014).
9. Lyu, H., Fan, Y., Hao, Z. & Wang, J. Effect of local and general fatiguing exercises on disturbed and static postural control. *J. Electromyogr. Kinesiol.* **56**, 102487 (2021).
10. Semmler, J. G., Ebert, S. A. & Amarasena, J. Eccentric muscle damage increases intermuscular coherence during a fatiguing isometric contraction. *Acta Physiol.* **208**, 362–375 (2013).
11. Halliday, D. M. & Rosenberg, J. R. On the application, estimation and interpretation of coherence and pooled coherence. *J. Neurosci. Methods* **100**, 173–174 (2000).
12. Grosse, P., Cassidy, M. J. & Brown, P. EEG–EMG, MEG–EMG and EMG–EMG frequency analysis: physiological principles and clinical applications. *Clin. Neurophysiol.* **113**, 1523–1531 (2002).
13. Maatar, D., Fournier, R., Lachiri, Z. & Nait-Ali, A. Discrete wavelet and modified PCA decompositions for postural stability analysis in biometric applications. *J. Biomed. Sci. Eng.* **4**, 543–551 (2011).
14. Ismail, A. R. & Asfour, S. S. Discrete wavelet transform: a tool in smoothing kinematic data. *J. Biomech.* **32**, 317–321 (1999).

15. Enoka, R. M. & Duchateau, J. Muscle fatigue: what, why and how it influences muscle function. *J. Physiol.* **586**, 11–23 (2008).
16. Paillard, T. Effects of general and local fatigue on postural control: A review. *Neurosci. Biobehav. Rev.* **36**, 162–176 (2012).
17. Remaud, A., Thuong-Cong, C. & Bilodeau, M. Age-Related Changes in Dynamic Postural Control and Attentional Demands are Minimally Affected by Local Muscle Fatigue. *Front. Aging Neurosci.* **7**, 257 (2016).
18. Jo, D. *et al.* Sex differences in the effect of muscle fatigue on static postural control under different vision and task conditions. *PLOS ONE* **17**, e0269705 (2022).
19. Bermejo, J. L. *et al.* The difficulty of postural tasks amplifies the effects of fatigue on postural stability. *Eur. J. Appl. Physiol.* **115**, 489–495 (2015).
20. Liang, Z., Clark, R., Bryant, A., Quek, J. & Pua, Y. H. Neck musculature fatigue affects specific frequency bands of postural dynamics during quiet standing. *Gait Posture* **39**, 397–403 (2014).
21. Collins, J. J. & De Luca, C. J. Open-loop and closed-loop control of posture: a random-walk analysis of center-of-pressure trajectories. *Exp. Brain Res.* **95**, 308–318 (1993).
22. Loram, I. D., Maganaris, C. N. & Lakie, M. The passive, human calf muscles in relation to standing: the non-linear decrease from short range to long range stiffness. *J. Physiol.* **584**, 661–675 (2007).
23. Ojha, A., Alderink, G. & Rhodes, S. Coherence between electromyographic signals of anterior tibialis, soleus, and gastrocnemius during standing balance tasks. *Front. Hum. Neurosci.* **17**, 1042758 (2023).
24. Laine, C. M. & Valero-Cuevas, F. J. Intermuscular coherence reflects functional coordination. *J. Neurophysiol.* **118**, 1775–1783 (2017).
25. Reynolds, R. F., Liedtke, A. M. & Lakie, M. Intrinsic ankle stiffness is associated with paradoxical calf muscle movement but not postural sway or age. *Exp. Physiol.* **109**, 729–737 (2024).
26. Nashner, L. M. & McCollum, G. The organization of human postural movements: A formal basis and experimental synthesis. *Behav. Brain Sci.* **8**, 135–150 (1985).
27. Shorter, A. L. *et al.* Characterization and clinical implications of ankle impedance during walking in chronic stroke. *Sci. Rep.* **11**, 16726 (2021).
28. Franklin, D. W., Osu, R., Burdet, E., Kawato, M. & Milner, T. E. Adaptation to stable and unstable dynamics achieved by combined impedance control and inverse dynamics model. *J. Neurophysiol.* **90**, 3270–3282 (2003).
29. Nielsen, J. & Kagamihara, Y. The regulation of disynaptic reciprocal Ia inhibition during co-contraction of antagonistic muscles in man. *J. Physiol.* **456**, 373–391 (1992).
30. Falconer, K. & Winter, D. A. Quantitative assessment of co-contraction at the ankle joint in walking. *Electromyogr. Clin. Neurophysiol.* **25**, 135–149 (1985).

31. Kim, D. & Hwang, J.-M. The center of pressure and ankle muscle co-contraction in response to anterior-posterior perturbations. *PLoS ONE* **13**, e0207667 (2018).
32. Falk, J. *et al.* Increased co-contraction reaction during a surface perturbation is associated with unsuccessful postural control among older adults. *BMC Geriatr.* **22**, 438 (2022).
33. Warnica, M. J., Weaver, T. B., Prentice, S. D. & Laing, A. C. The influence of ankle muscle activation on postural sway during quiet stance. *Gait Posture* **39**, 1115–1121 (2014).
34. Donath, L., Kurz, E., Roth, R., Zahner, L. & Faude, O. Different ankle muscle coordination patterns and co-activation during quiet stance between young adults and seniors do not change after a bout of high intensity training. *BMC Geriatr.* **15**, 19 (2015).
35. Quijoux, F. *et al.* A review of center of pressure (COP) variables to quantify standing balance in elderly people: Algorithms and open-access code*. *Physiol. Rep.* **9**, (2021).
36. Vette, A. H. *et al.* Ankle muscle co-contractions during quiet standing are associated with decreased postural steadiness in the elderly. *Gait Posture* **55**, 31–36 (2017).
37. Carpenter, M., Frank, J., Silcher, C. & Peysar, G. The influence of postural threat on the control of upright stance. *Exp. Brain Res.* **138**, 210–218 (2001).
38. Hansen, S., Hansen, N. L., Christensen, L. O. D., Petersen, N. T. & Nielsen, J. B. Coupling of antagonistic ankle muscles during co-contraction in humans. *Exp. Brain Res.* **146**, 282–292 (2002).
39. Thompson, J. D., Plummer, P. & Franz, J. R. Age and falls history effects on antagonist leg muscle coactivation during walking with balance perturbations. *Clin. Biomech. Bristol Avon* **59**, 94–100 (2018).
40. Carty, C. P. *et al.* Reactive stepping behaviour in response to forward loss of balance predicts future falls in community-dwelling older adults. *Age Ageing* **44**, 109–115 (2015).
41. Jacobi, H. *et al.* Dual task effect on postural control in patients with degenerative cerebellar disorders. *Cerebellum Ataxias* **2**, 6 (2015).
42. Lang, K. C., Hackney, M. E., Ting, L. H. & McKay, J. L. Antagonist muscle activity during reactive balance responses is elevated in Parkinson's disease and in balance impairment. *PloS One* **14**, e0211137 (2019).
43. Nelson-Wong, E. *et al.* Increased fall risk is associated with elevated co-contraction about the ankle during static balance challenges in older adults. *Eur. J. Appl. Physiol.* **112**, 1379–1389 (2012).
44. Boonstra, T. W. & Breakspear, M. Neural mechanisms of intermuscular coherence: implications for the rectification of surface electromyography. *J. Neurophysiol.* **107**, 796–807 (2012).
45. Nandi, T., Hortobágyi, T., van Keeken, H. G., Salem, G. J. & Lamoth, C. J. C. Standing task difficulty related increase in agonist-agonist and agonist-antagonist common inputs are driven by corticospinal and subcortical inputs respectively. *Sci. Rep.* **9**, 2439 (2019).

46. McManus, L., Hu, X., Rymer, W. Z., Suresh, N. L. & Lowery, M. M. Muscle fatigue increases beta-band coherence between the firing times of simultaneously active motor units in the first dorsal interosseous muscle. *J. Neurophysiol.* **115**, 2830–2839 (2016).
47. Fisher, K. M., Zaaimi, B., Williams, T. L., Baker, S. N. & Baker, M. R. Beta-band intermuscular coherence: a novel biomarker of upper motor neuron dysfunction in motor neuron disease. *Brain* **135**, 2849–2864 (2012).
48. Aguiar, S. A., Baker, S. N., Gant, K., Bohorquez, J. & Thomas, C. K. Spasms after spinal cord injury show low-frequency intermuscular coherence. *J. Neurophysiol.* **120**, 1765–1771 (2018).
49. Obata, H., Abe, M. O., Masani, K. & Nakazawa, K. Modulation between bilateral legs and within unilateral muscle synergists of postural muscle activity changes with development and aging. *Exp. Brain Res.* **232**, 1–11 (2014).
50. Boonstra, T. W. *et al.* Muscle networks: Connectivity analysis of EMG activity during postural control. *Sci. Rep.* **5**, 17830 (2015).
51. Yamanaka, E., Horiuchi, Y. & Nojima, I. EMG-EMG coherence during voluntary control of human standing tasks: a systematic scoping review. *Front. Neurosci.* **17**, 1187716 (2023).
52. Wang, L. *et al.* Fatigue-related electromyographic coherence and phase synchronization analysis between antagonistic elbow muscles. *Exp. Brain Res.* **233**, 971–982 (2015).
53. Alexandrov, A. V., Frolov, A. A., Horak, F. B., Carlson-Kuhta, P. & Park, S. Feedback equilibrium control during human standing. *Biol. Cybern.* **93**, 309–322 (2005).
54. Santos, M. J., Kanekar, N. & Aruin, A. S. The role of anticipatory postural adjustments in compensatory control of posture: 2. Biomechanical analysis. *J. Electromyogr. Kinesiol.* **20**, 398–405 (2010).
55. Chagdes, J. R. *et al.* Multiple timescales in postural dynamics associated with vision and a secondary task are revealed by wavelet analysis. *Exp. Brain Res.* **197**, 297–310 (2009).
56. Klous, M., Mikulic, P. & Latash, M. L. Two aspects of feedforward postural control: anticipatory postural adjustments and anticipatory synergy adjustments. *J. Neurophysiol.* **105**, 2275–2288 (2011).
57. Mello, R. G. T., Oliveira, L. F. & Nadal, J. Anticipation mechanism in body sway control and effect of muscle fatigue. *J. Electromyogr. Kinesiol.* **17**, 739–746 (2007).
58. Iwamoto, Y., Takahashi, M. & Shinkoda, K. Differences of muscle co-contraction of the ankle joint between young and elderly adults during dynamic postural control at different speeds. *J. Physiol. Anthropol.* **36**, 32 (2017).
59. Maki, B. E., Holliday, P. J. & Topper, A. K. A prospective study of postural balance and risk of falling in an ambulatory and independent elderly population. *J. Gerontol.* **49**, M72-84 (1994).

60. Boyas, S., Remaud, A., Rivers, E. & Bilodeau, M. Fatiguing Exercise Intensity Influences the Relationship between Parameters Reflecting Neuromuscular Function and Postural Control Variables. *PLoS ONE* **8**, e72482 (2013).
61. Peterka, R. J. Sensorimotor Integration in Human Postural Control. *J. Neurophysiol.* **88**, 1097–1118 (2002).
62. Bronstein, A. M. Multisensory integration in balance control. *Handb. Clin. Neurol.* **137**, 57–66 (2016).
63. Grace Gaerlan, M., Alpert, P. T., Cross, C., Louis, M. & Kowalski, S. Postural balance in young adults: The role of visual, vestibular and somatosensory systems. *J. Am. Acad. Nurse Pract.* **24**, 375–381 (2012).
64. Cullen, K. E. The vestibular system: multimodal integration and encoding of self-motion for motor control. *Trends Neurosci.* **35**, 185–196 (2012).
65. Day, B. L. & Cole, J. Vestibular-evoked postural responses in the absence of somatosensory information. *Brain J. Neurol.* **125**, 2081–2088 (2002).
66. Horak, F. B. Postural orientation and equilibrium: what do we need to know about neural control of balance to prevent falls? *Age Ageing* **35**, ii7–ii11 (2006).
67. Assländer, L. & Peterka, R. J. Sensory reweighting dynamics in human postural control. *J. Neurophysiol.* **111**, 1852–1864 (2014).
68. Norton, J. A. & Gorassini, M. A. Changes in Cortically Related Intermuscular Coherence Accompanying Improvements in Locomotor Skills in Incomplete Spinal Cord Injury. *J. Neurophysiol.* **95**, 2580–2589 (2006).
69. Liu, J., Sheng, Y. & Liu, H. Corticomuscular Coherence and Its Applications: A Review. *Front. Hum. Neurosci.* **13**, 100 (2019).
70. Gribble, P. A. & Hertel, J. Effect of lower-extremity muscle fatigue on postural control. *Arch. Phys. Med. Rehabil.* **85**, 589–592 (2004).
71. Oie, K. S., Kiemel, T. & Jeka, J. J. Multisensory fusion: simultaneous re-weighting of vision and touch for the control of human posture. *Cogn. Brain Res.* **14**, 164–176 (2002).
72. Sim, T. *et al.* Analysis of sensory system aspects of postural stability during quiet standing in adolescent idiopathic scoliosis patients. *J. NeuroEngineering Rehabil.* **15**, 54 (2018).
73. Rizzato, A. *et al.* Different neuromuscular control mechanisms regulate static and dynamic balance: A center-of-pressure analysis in young adults. *Hum. Mov. Sci.* **90**, 103120 (2023).
74. Richmond, S. B., Fling, B. W., Lee, H. & Peterson, D. S. The assessment of center of mass and center of pressure during quiet stance: Current applications and future directions. *J. Biomech.* **123**, 110485 (2021).

75. Carpenter, M. G., Murnaghan, C. D. & Inglis, J. T. Shifting the balance: evidence of an exploratory role for postural sway. *Neuroscience* **171**, 196–204 (2010).
76. Zatsiorsky, V. M. & Duarte, M. Instant Equilibrium Point and Its Migration in Standing Tasks: Rambling and Trembling Components of the Stabilogram. *Motor Control* **3**, 28–38 (1999).
77. Richer, N. & Lajoie, Y. Automaticity of Postural Control while Dual-tasking Revealed in Young and Older Adults. *Exp. Aging Res.* **46**, 1–21 (2020).
78. Gerber, E. D., Huang, C.-K., Moon, S., Devos, H. & Luchies, C. W. Sensory reweighting of postural control requires distinct rambling and trembling sway adaptations. *Gait Posture* **112**, 16–21 (2024).
79. Quek, J., Brauer, S. G., Clark, R. & Treleaven, J. New insights into neck-pain-related postural control using measures of signal frequency and complexity in older adults. *Gait Posture* **39**, 1069–1073 (2014).
80. Paillard, T., Costes-Salon, C., Lafont, C. & Dupui, P. Are there differences in postural regulation according to the level of competition in judoists? *Br. J. Sports Med.* **36**, 304–305 (2002).
81. Kubota, K. *et al.* Muscle co-activation in the elderly contributes to control of hip and knee joint torque and endpoint force. *Sci. Rep.* **13**, 7139 (2023).
82. Kennedy, A., Hug, F., Bilodeau, M., Sveistrup, H. & Guével, A. Neuromuscular fatigue induced by alternating isometric contractions of the ankle plantar and dorsiflexors. *J. Electromyogr. Kinesiol.* **21**, 471–477 (2011).
83. Abd-Elfattah, H. M., Abdelazeim, F. H. & Elshennawy, S. Physical and cognitive consequences of fatigue: A review. *J. Adv. Res.* **6**, 351–358 (2015).
84. Vuillerme, N., Danion, F., Forestier, N. & Nougier, V. Postural sway under muscle vibration and muscle fatigue in humans. *Neurosci. Lett.* **333**, 131–135 (2002).
85. Abutaleb, E. E. & Mohamed, A. H. Effect of induced fatigue on dynamic postural balance in healthy young adults. *Bull. Fac. Phys. Ther.* **20**, 161–167 (2015).
86. Boyas, S., Hajj, M. & Bilodeau, M. Influence of ankle plantarflexor fatigue on postural sway, lower limb articular angles, and postural strategies during unipedal quiet standing. *Gait Posture* **37**, 547–551 (2013).
87. Corbeil, P., Blouin, J.-S., Bégin, F., Nougier, V. & Teasdale, N. Perturbation of the postural control system induced by muscular fatigue. *Gait Posture* **18**, 92–100 (2003).
88. Roerdink, M., Hlavackova, P. & Vuillerme, N. Effects of plantar-flexor muscle fatigue on the magnitude and regularity of center-of-pressure fluctuations. *Exp. Brain Res.* **212**, 471–476 (2011).
89. Bisson, E. J., Lajoie, Y. & Bilodeau, M. The influence of age and surface compliance on changes in postural control and attention due to ankle neuromuscular fatigue. *Exp. Brain Res.* **232**, 837–845 (2014).

90. Yaggie, J. A. & McGregor, S. J. Effects of isokinetic ankle fatigue on the maintenance of balance and postural limits. *Arch. Phys. Med. Rehabil.* **83**, 224–228 (2002).
91. Jo, D. & Bilodeau, M. Sex differences concerning the effects of ankle muscle fatigue on static postural control and spinal proprioceptive input at the ankle. *Front. Hum. Neurosci.* **17**, 1015597 (2023).
92. Du, Y. & Fan, Y. The Effect of Fatigue on Postural Control and Biomechanical Characteristic of Lunge in Badminton Players. *Bioengineering* **10**, 301 (2023).
93. Vuillerme, N., Burdet, C., Isableu, B. & Demetz, S. The magnitude of the effect of calf muscles fatigue on postural control during bipedal quiet standing with vision depends on the eye-visual target distance. *Gait Posture* **24**, 169–172 (2006).
94. Barbieri, F. A. *et al.* Effects of Ankle Muscle Fatigue and Visual Behavior on Postural Sway in Young Adults. *Front. Physiol.* **10**, 643 (2019).
95. Koyama, K. & Yamauchi, J. Altered postural sway following fatiguing foot muscle exercises. *PLoS ONE* **12**, e0189184 (2017).
96. Vuillerme, N., Nougier, V. & Prieur, J.-M. Can vision compensate for a lower limbs muscular fatigue for controlling posture in humans? *Neurosci. Lett.* **308**, 103–106 (2001).
97. Caron, O. Effects of local fatigue of the lower limbs on postural control and postural stability in standing posture. *Neurosci. Lett.* **340**, 83–86 (2003).
98. Sun, Y., Sun, Y., Zhang, J. & Ran, F. Sensor-Based Assessment of Mental Fatigue Effects on Postural Stability and Multi-Sensory Integration. *Sensors* **25**, 1470 (2025).
99. Hoseinpoor, T. S., Kahrizi, S. & Mobini, B. Trunk extensor muscle fatigue influences trunk muscle activities. *Work* **51**, 793–797 (2015).
100. Rinaldin, C. D. P. *et al.* Compensatory control between the legs in automatic postural responses to stance perturbations under single-leg fatigue. *Exp. Brain Res.* **239**, 639–653 (2021).
101. Kennedy, A., Guevel, A. & Sveistrup, H. Impact of ankle muscle fatigue and recovery on the anticipatory postural adjustments to externally initiated perturbations in dynamic postural control. *Exp. Brain Res.* **223**, 553–562 (2012).
102. Penedo, T. *et al.* Motor strategy during postural control is not muscle fatigue joint-dependent, but muscle fatigue increases postural asymmetry. *PLOS ONE* **16**, e0247395 (2021).
103. Chang, Y.-J. *et al.* Increases of quadriceps inter-muscular cross-correlation and coherence during exhausting stepping exercise. *Sensors* **12**, 16353–16367 (2012).
104. Castronovo, A. M., De Marchis, C., Schmid, M., Conforto, S. & Severini, G. Effect of Task Failure on Intermuscular Coherence Measures in Synergistic Muscles. *Appl. Bionics Biomech.* **2018**, 4759232 (2018).

105. Danna-Dos Santos, A. *et al.* Influence of Fatigue on Hand Muscle Coordination and EMG-EMG Coherence During Three-Digit Grasping. *J. Neurophysiol.* **104**, 3576–3587 (2010).
106. Rudolph, K. S., Axe, M. J. & Snyder-Mackler, L. Dynamic stability after ACL injury: who can hop? *Knee Surg. Sports Traumatol. Arthrosc.* **8**, 262–269 (2000).
107. Yao, B., Salenius, S., Yue, G. H., Brown, R. W. & Liu, J. Z. Effects of surface EMG rectification on power and coherence analyses: An EEG and MEG study. *J. Neurosci. Methods* **159**, 215–223 (2007).
108. Terry, K. & Griffin, L. How computational technique and spike train properties affect coherence detection. *J. Neurosci. Methods* **168**, 212–223 (2008).
109. Singer, J. C. & Mochizuki, G. Post-Stroke Lower Limb Spasticity Alters the Interlimb Temporal Synchronization of Centre of Pressure Displacements Across Multiple Timescales. *IEEE Trans. Neural Syst. Rehabil. Eng.* **23**, 786–795 (2015).
110. Wodarski, P., Jurkojć, J. & Gzik, M. Wavelet Decomposition in Analysis of Impact of Virtual Reality Head Mounted Display Systems on Postural Stability. *Sensors* **20**, 7138 (2020).
111. Gow, B. J., Peng, C.-K., Wayne, P. M. & Ahn, A. C. Multiscale Entropy Analysis of Center-of-Pressure Dynamics in Human Postural Control: Methodological Considerations. *Entropy* **17**, 7926–7947 (2015).
112. Ruhe, A., Fejer, R. & Walker, B. The test-retest reliability of centre of pressure measures in bipedal static task conditions--a systematic review of the literature. *Gait Posture* **32**, 436–445 (2010).
113. Jafari, H., Gustafsson, T., Nyberg, L. & Röijezon, U. Predicting balance impairments in older adults: a wavelet-based center of pressure classification approach. *Biomed. Eng. OnLine* **22**, 83 (2023).
114. Boonstra, T. W. *et al.* Fatigue-related changes in motor-unit synchronization of quadriceps muscles within and across legs. *J. Electromyogr. Kinesiol.* **18**, 717–731 (2008).
115. Singh, T. & Latash, M. L. EFFECTS OF MUSCLE FATIGUE ON MULTI-MUSCLE SYNERGIES. *Exp. Brain Res. Exp. Hirnforsch. Exp. Cerebrale* **214**, 335–350 (2011).
116. Ridge, S. T. *et al.* Contributions of Intrinsic and Extrinsic Foot Muscles during Functional Standing Postures. *BioMed Res. Int.* **2022**, 7708077 (2022).
117. Martino, G., Beck, O. N. & Ting, L. H. Voluntary muscle coactivation in quiet standing elicits reciprocal rather than coactive agonist-antagonist control of reactive balance. *J. Neurophysiol.* **129**, 1378–1388 (2023).
118. Sinha, T. & Maki, B. E. Effect of forward lean on postural ankle dynamics. *IEEE Trans. Rehabil. Eng. Publ. IEEE Eng. Med. Biol. Soc.* **4**, 348–359 (1996).
119. Braun Ferreira, L. A. *et al.* Analysis of electromyographic activity of ankle muscles on stable and unstable surfaces with eyes open and closed. *J. Bodyw. Mov. Ther.* **15**, 496–501 (2011).

120. Granacher, U., Gruber, M., Förderer, D., Strass, D. & Gollhofer, A. Effects of ankle fatigue on functional reflex activity during gait perturbations in young and elderly men. *Gait Posture* **32**, 107–112 (2010).
121. Smart, R. R. *et al.* Intermuscular coherence of plantar and dorsiflexor muscles in older adults with Parkinson's disease and age-matched controls during bipedal and unipedal stance. *Front. Aging Neurosci.* **15**, 1207283 (2023).
122. Wang, L.-J. *et al.* Muscle Fatigue Enhance Beta Band EMG-EMG Coupling of Antagonistic Muscles in Patients With Post-stroke Spasticity. *Front. Bioeng. Biotechnol.* **8**, 1011 (2020).
123. Kattla, S. & Lowery, M. M. Fatigue related changes in electromyographic coherence between synergistic hand muscles. *Exp. Brain Res.* **202**, 89–99 (2010).
124. Farina, D. *et al.* The extraction of neural information from the surface EMG for the control of upper-limb prostheses: emerging avenues and challenges. *IEEE Trans. Neural Syst. Rehabil. Eng. Publ. IEEE Eng. Med. Biol. Soc.* **22**, 797–809 (2014).
125. Jacobs, J. V. & Horak, F. B. Cortical control of postural responses. *J. Neural Transm. Vienna Austria 1996* **114**, 1339–1348 (2007).
126. Maurer, C. & Peterka, R. J. A New Interpretation of Spontaneous Sway Measures Based on a Simple Model of Human Postural Control. *J. Neurophysiol.* **93**, 189–200 (2005).
127. Myers, L. J., Erim, Z. & Lowery, M. M. Time and frequency domain methods for quantifying common modulation of motor unit firing patterns. *J. NeuroEngineering Rehabil.* **1**, 2 (2004).
128. Mongold, S. J. *et al.* Aging-related changes in neuromuscular control strategies and their influence on postural stability. *Sci. Rep.* **15**, 30127 (2025).
129. Cleworth, T. W. *et al.* Postural Threat Modulates Perceptions of Balance-Related Movement During Support Surface Rotations. *Neuroscience* **404**, 413–422 (2019).
130. Marchant, D. C. Attentional Focusing Instructions and Force Production. *Front. Psychol.* **1**, 210 (2011).
131. da Silva, M. C. *et al.* Effects of Fatigue on Postural Sway and Electromyography Modulation in Young Expert Acrobatic Gymnasts and Healthy Non-trained Controls During Unipedal Stance. *Front. Physiol.* **13**, 782-838 (2022).
132. Kozinc, Ž., Trajković, N., Smajla, D. & Šarabon, N. The Effect of Fatigue on Single-Leg Postural Sway and Its Transient Characteristics in Healthy Young Adults. *Front. Physiol.* **12**, 720-905 (2021).
133. Rojhani-Shirazi, Z., Amiri, Z. & Ebrahimi, S. Effects of Plantar Flexor Muscles Fatigue on Postural Control during Quiet Stance and External Perturbation in Healthy Subjects. J. Biomed. Phys. Eng. 9, 729–738 (2019).

134. Jang, Y. I., Sim, J. Y., Yang, J.-R. & Kwon, N. K. The Optimal Selection of Mother Wavelet Function and Decomposition Level for Denoising of DCG Signal. *Sensors* **21**, 1851 (2021).
135. Nojima, I., Watanabe, T., Saito, K., Tanabe, S. & Kanazawa, H. Modulation of EMG-EMG Coherence in a Choice Stepping Task. *Front. Hum. Neurosci.* **12**, 50 (2018).
136. Duarte, M. & Zatsiorsky, V. M. On the fractal properties of natural human standing. *Neurosci. Lett.* **283**, 173–176 (2000).
137. Houdijk, H., Brown, S. E. & van Dieën, J. H. Relation between postural sway magnitude and metabolic energy cost during upright standing on a compliant surface. *J. Appl. Physiol.* **119**, 696–703 (2015).
138. Kiemel, T., Oie, K. S. & Jeka, J. J. The slow dynamics of postural sway are in the feedback loop. *J. Neurophysiol.* **95**, 1410–1418 (2006).
139. Pasma, J. H. *et al.* Changes in sensory reweighting of proprioceptive information during standing balance with age and disease. *J. Neurophysiol.* **114**, 3220–3233 (2015).
140. Murnaghan, C. D., Horslen, B. C., Inglis, J. T. & Carpenter, M. G. Exploratory behavior during stance persists with visual feedback. *Neuroscience* **195**, 54–59 (2011).
141. Michaud, L., Lafleur, D. & Lajoie, Y. Effect of Center of Mass Immobilization on Center of Pressure Displacement in Single and Dual-Task. *J. Mot. Behav.* **55**, 539–549 (2023).
142. Button, K. S. *et al.* Power failure: why small sample size undermines the reliability of neuroscience. *Nat. Rev. Neurosci.* **14**, 365–376 (2013).
143. Stergiou, N. & Decker, L. M. Human movement variability, nonlinear dynamics, and pathology: Is there a connection? Hum. Mov. Sci. 30, 869–888 (2011).

# Appendix A

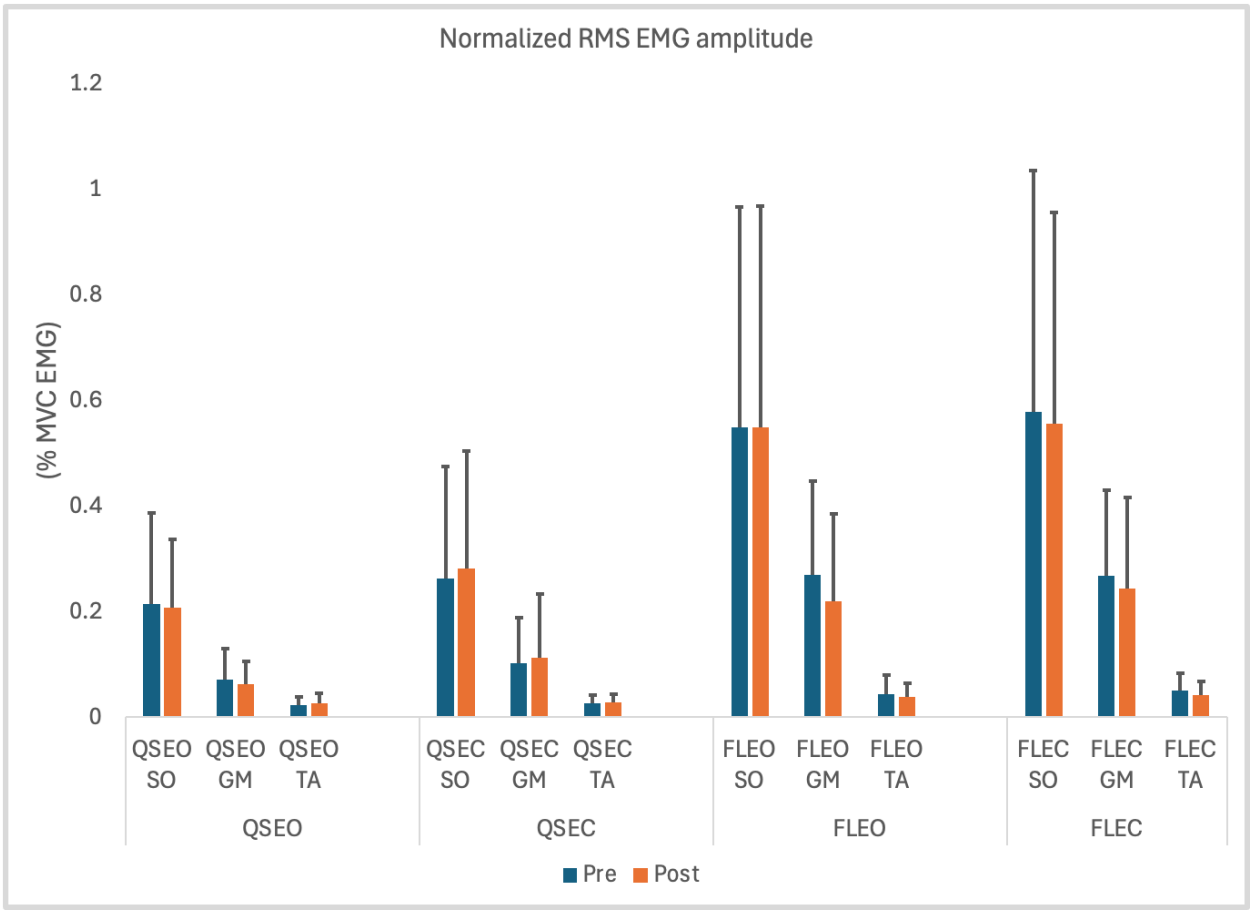


Figure A1: EMG RMS amplitude for all three muscles in all conditions normalized to pre-fatigue MVC EMG RMS value.

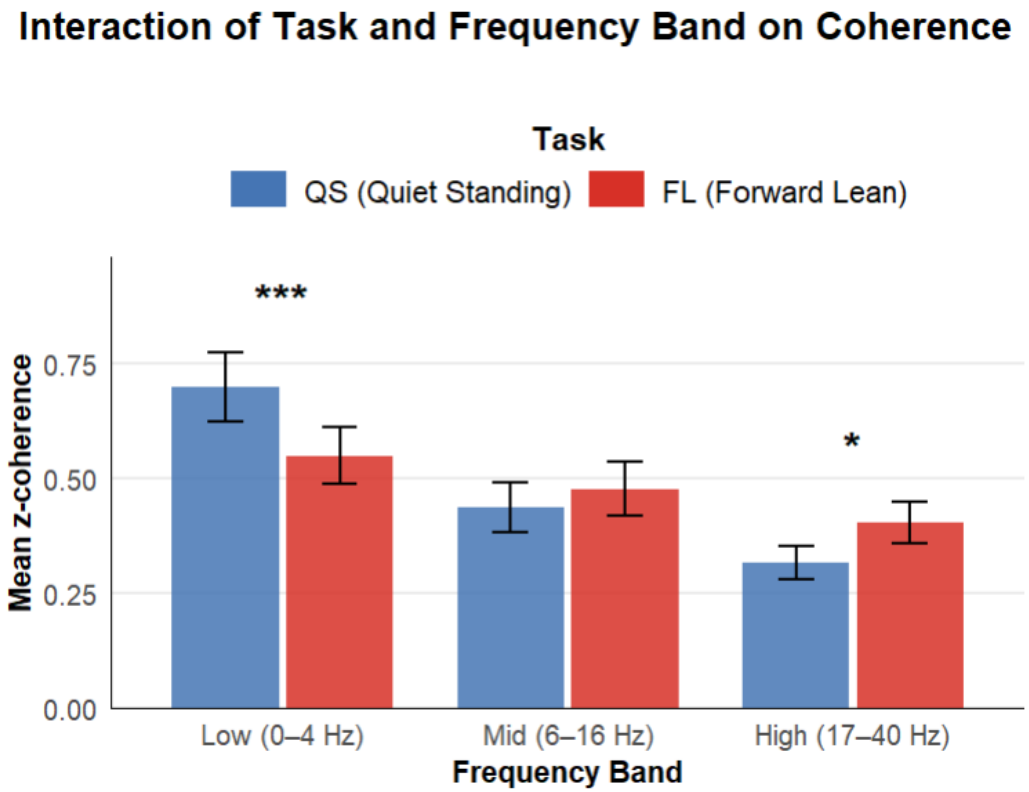


Figure A2: Mean (± SE) pooled z-transformed AG-AG (SOL-GM) intermuscular coherence across low (0‑4 Hz), mid (6‑16 Hz), and high (17‑40 Hz) frequency bands for Quiet Standing (QS; blue) and Forward Lean (FL; red) tasks.

Table A1: Post-hoc simple-effects contrasts testing Eyes Closed vs. Eyes Open (EC − EO) within each postural task for each frequency band in AG-AG. Values are model-based estimated marginal mean contrasts on Fisher z-transformed coherence (Estimate ± SE, 95% CI) with Bonferroni-adjusted p-values. Degrees of freedom reflect the repeated-measures model (df = 12; n = 13).

| Frequency band (Hz) | Contrast (EC – EO) | df | Estimate (z) | SE | 95% CI | t | p (Bonferroni) |
|---|---|---|---|---|---|---|---|
| *Low (0–3.94)* | QSEC – QSEO | 12 | −0.1285 | 0.0236 | [−0.1890, −0.0680] | −5.440 | <.001*** |
| | FLEC – FLEO | 12 | −0.1600 | 0.0429 | [−0.2698, −0.0502] | −3.731 | 0.006** |
| *Mid (5.92–15.78)* | QSEC – QSEO | 12 | −0.0513 | 0.0167 | [−0.0940, −0.0086] | −3.073 | 0.019* |
| | FLEC – FLEO | 12 | −0.0862 | 0.0298 | [−0.1624, −0.0100] | −2.896 | 0.027* |
| *High (17.75–39.45)* | QSEC – QSEO | 12 | −0.0394 | 0.0123 | [−0.0710, −0.0079] | −3.198 | 0.015* |
| | FLEC – FLEO | 12 | −0.0647 | 0.02 | [−0.1160, −0.0134] | −3.231 | 0.014* |

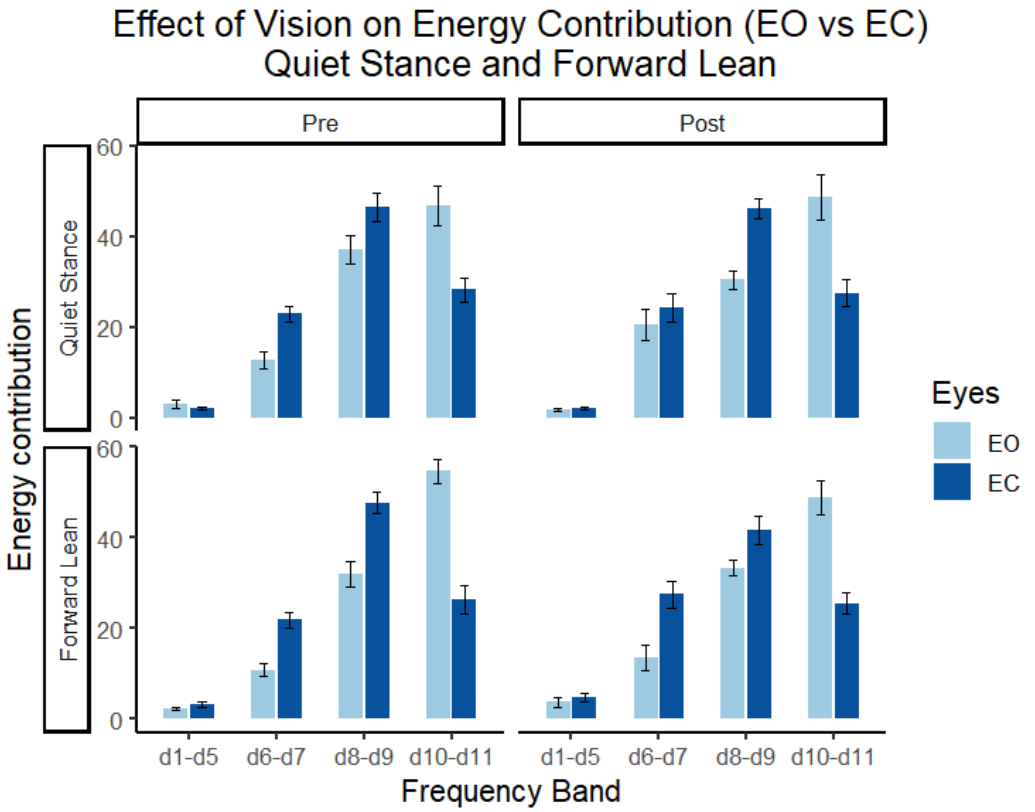


Figure A3: (±SE) energy contribution across frequency bands (d1–d5, d6–d7, d8–d9, d10–d11) during Quiet Stance and Forward Lean, shown separately for Pre and Post conditions in AP plane. Bars depict group means; error bars indicate the standard error. Light blue = Eyes Open (EO); dark blue = Eyes Closed (EC). Values represent the percentage contribution of band-limited energy (DWT-based) to total sway energy.

Table A2: Pooled post-hoc differences between Quiet Stance and Forward Lean (QS − FL) across frequency bands and vision conditions.

| Differences Between Quiet Stance and Forward Lean | | | | | | |
|---|---|---|---|---|---|---|
| **Band** | **Vision** | **Estimate** | **SE** | **df** | **t ratio** | **p value** |
| *d1-d5* | Eyes open | −0.6325 | 0.7462 | 13 | −0.848 | 0.412 |
| *d6-d7* | Eyes open | 4.4295 | 1.9368 | 13 | 2.287 | **0.0396** |
| *d8-d9* | Eyes open | 1.1482 | 2.2347 | 13 | 0.514 | 0.616 |
| *d10-d11* | Eyes open | −4.0088 | 3.2251 | 13 | −1.243 | 0.2358 |
| *d1-d5* | Eyes closed | −1.8914 | 0.528 | 13 | −3.582 | **0.0033** |
| *d6-d7* | Eyes closed | −1.0102 | 3.0656 | 13 | −0.330 | 0.747 |
| *d8-d9* | Eyes closed | 1.6916 | 3.4661 | 13 | 0.488 | 0.6336 |
| *d10-d11* | Eyes closed | 1.985 | 3.5559 | 13 | 0.558 | 0.5862 |

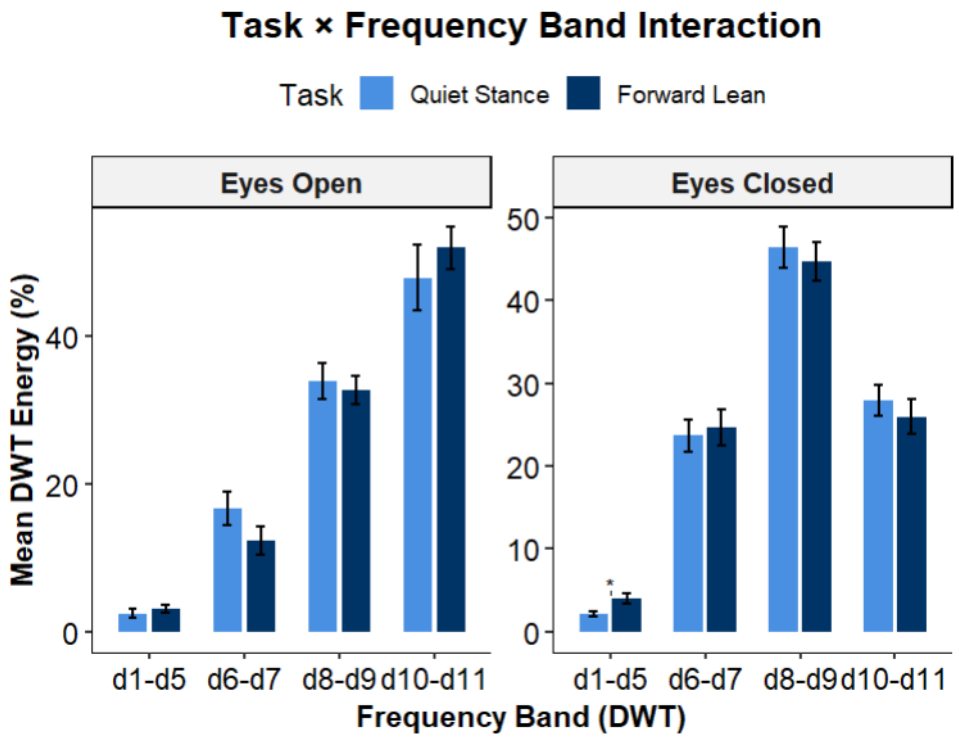


Figure A4: Mean (± SE) Discrete wavelet transformation energy levels for eyes-open and eyes-closed across open loop (d1-d5), proprioceptive (d6-d7), vestibular (d8-d9) and visual (d10-d11) frequency bands for Quiet Standing (QS; blue) and Forward Lean (FL; red) tasks.

Table A3: Pearson correlation coefficients (r) and p-values between AG–AG coherence bands and relative energy in DWT bands for a pre fatigue state. Differences in coherence in pre fatigue were not systematically associated with changes in DWT energy across sensory modalities, with most correlations failing to reach significance ($p > .05$).

| Pre AG-AG Coherence bands | Task | Open loop | | Somatosensory | | Vestibular | | Visual | |
|---|---|---|---|---|---|---|---|---|---|
| | | r | p | r | p | r | p | r | p |
| *Low (0-3.94 Hz)* | QSEO | 0.245 | 0.419 | -0.226 | 0.458 | -0.592* | 0.033 | 0.454 | 0.119 |
| *Mid (5.92-15.78 Hz)* | QSEO | -0.105 | 0.732 | 0.103 | 0.739 | -0.11 | 0.72 | 0.052 | 0.867 |
| *High (17.75-39.45 Hz)* | QSEO | -0.099 | 0.747 | 0.155 | 0.613 | -0.127 | 0.678 | 0.04 | 0.896 |
| *Low (0-3.94 Hz)* | QSEC | 0.075 | 0.798 | 0.08 | 0.786 | -0.052 | 0.86 | -0.001 | 0.998 |
| *Mid (5.92-15.78 Hz)* | QSEC | 0.069 | 0.814 | 0.018 | 0.95 | -0.037 | 0.9 | 0.022 | 0.942 |
| *High (17.75-39.45 Hz)* | QSEC | 0.213 | 0.464 | 0.006 | 0.984 | 0.241 | 0.407 | -0.318 | 0.268 |
| *Low (0-3.94 Hz)* | FLEO | -0.024 | 0.935 | -0.011 | 0.969 | -0.321 | 0.263 | 0.355 | 0.213 |
| *Mid (5.92-15.78 Hz)* | FLEO | 0.124 | 0.673 | 0.15 | 0.609 | -0.522 | 0.056 | 0.472 | 0.088 |
| *High (17.75-39.45 Hz)* | FLEO | 0.149 | 0.612 | 0.048 | 0.869 | -0.479 | 0.083 | 0.48 | 0.083 |
| *Low (0-3.94 Hz)* | FLEC | 0.357 | 0.21 | 0.287 | 0.32 | -0.005 | 0.986 | -0.14 | 0.634 |
| *Mid (5.92-15.78 Hz)* | FLEC | 0.224 | 0.441 | 0.124 | 0.673 | -0.112 | 0.704 | 0.05 | 0.866 |
| *High (17.75-39.45 Hz)* | FLEC | 0.231 | 0.427 | -0.028 | 0.923 | 0.007 | 0.981 | 0.048 | 0.871 |

Table A4: Pearson correlation coefficients (r) and p-values between AG–AG coherence bands and relative energy in DWT bands for a post fatigue state. Differences in coherence in post fatigue were not systematically associated with changes in DWT energy across sensory modalities, with most correlations failing to reach significance ($p > .05$).

| Post AG-AG Coherence bands | Task | Open loop | | Somatosensory | | Vestibular | | Visual | |
|---|---|---|---|---|---|---|---|---|---|
| | | r | p | r | p | r | p | r | p |
| *Low (0-3.94 Hz)* | QSEO | 0.41 | 0.165 | -0.035 | 0.911 | -0.076 | 0.805 | 0.159 | 0.603 |
| *Mid (5.92-15.78 Hz)* | QSEO | 0.051 | 0.867 | -0.314 | 0.296 | 0.068 | 0.826 | 0.253 | 0.405 |
| *High (17.75-39.45 Hz)* | QSEO | -0.164 | 0.593 | -0.417 | 0.156 | 0.031 | 0.92 | 0.268 | 0.376 |
| *Low (0-3.94 Hz)* | QSEC | 0.361 | 0.205 | 0.026 | 0.93 | -0.256 | 0.377 | 0.064 | 0.827 |
| *Mid (5.92-15.78 Hz)* | QSEC | 0.3 | 0.297 | -0.129 | 0.66 | -0.086 | 0.769 | 0.116 | 0.693 |
| *High (17.75-39.45 Hz)* | QSEC | 0.114 | 0.697 | -0.258 | 0.374 | -0.056 | 0.848 | 0.271 | 0.349 |
| *Low (0-3.94 Hz)* | FLEO | -0.428 | 0.127 | -0.202 | 0.488 | -0.333 | 0.245 | 0.426 | 0.129 |
| *Mid (5.92-15.78 Hz)* | FLEO | -0.308 | 0.284 | 0.029 | 0.921 | -0.354 | 0.214 | 0.226 | 0.438 |
| *High (17.75-39.45 Hz)* | FLEO | -0.251 | 0.386 | -0.07 | 0.813 | -0.223 | 0.444 | 0.225 | 0.44 |
| *Low (0-3.94 Hz)* | FLEC | 0.3 | 0.298 | 0.209 | 0.473 | -0.166 | 0.57 | -0.182 | 0.533 |
| *Mid (5.92-15.78 Hz)* | FLEC | 0.371 | 0.191 | 0.188 | 0.519 | -0.28 | 0.332 | -0.025 | 0.932 |
| *High (17.75-39.45 Hz)* | FLEC | 0.256 | 0.376 | -0.024 | 0.936 | -0.198 | 0.497 | 0.14 | 0.634 |

Table A5: Pearson correlation coefficients (r) and p-values between AG–ANT (GM–TA) coherence bands and relative energy in DWT bands for a pre fatigue state. Differences in coherence in pre fatigue were not systematically associated with changes in DWT energy across sensory modalities, with most correlations failing to reach significance ($p > .05$).

| Pre AG-ANT (GM-TA) Coherence bands | Task | Open loop | | Somatosensory | | Vestibular | | Visual | |
|---|---|---|---|---|---|---|---|---|---|
| | | r | p | r | p | r | p | r | p |
| *Low (0-3.94 Hz)* | QSEO | -0.14 | 0.682 | -0.098 | 0.774 | -0.052 | 0.879 | 0.112 | 0.742 |
| *Mid (5.92-15.78 Hz)* | QSEO | -0.176 | 0.605 | 0.116 | 0.735 | -0.039 | 0.909 | 0.014 | 0.968 |
| *High (17.75-39.45 Hz)* | QSEO | -0.067 | 0.846 | 0.26 | 0.441 | -0.081 | 0.813 | -0.043 | 0.9 |
| *Low (0-3.94 Hz)* | QSEC | 0.275 | 0.387 | 0.469 | 0.124 | -0.181 | 0.573 | -0.237 | 0.459 |
| *Mid (5.92-15.78 Hz)* | QSEC | 0.312 | 0.324 | 0.418 | 0.177 | -0.085 | 0.792 | -0.321 | 0.31 |
| *High (17.75-39.45 Hz)* | QSEC | 0.14 | 0.665 | -0.025 | 0.938 | 0.116 | 0.72 | -0.145 | 0.653 |
| *Low (0-3.94 Hz)* | FLEO | -0.416 | 0.179 | -0.169 | 0.6 | -0.093 | 0.774 | 0.22 | 0.492 |
| *Mid (5.92-15.78 Hz)* | FLEO | -0.309 | 0.329 | -0.016 | 0.96 | -0.379 | 0.224 | 0.438 | 0.154 |
| *High (17.75-39.45 Hz)* | FLEO | -0.235 | 0.462 | -0.059 | 0.855 | -0.312 | 0.323 | 0.384 | 0.218 |
| *Low (0-3.94 Hz)* | FLEC | -0.191 | 0.552 | 0.14 | 0.663 | -0.197 | 0.54 | 0.14 | 0.664 |
| *Mid (5.92-15.78 Hz)* | FLEC | -0.249 | 0.436 | 0.163 | 0.613 | -0.38 | 0.223 | 0.282 | 0.375 |
| *High (17.75-39.45 Hz)* | FLEC | -0.221 | 0.491 | 0.029 | 0.928 | -0.217 | 0.498 | 0.235 | 0.462 |

Table A6: Pearson correlation coefficients (r) and p-values between AG–ANT (GM–TA) coherence bands and relative energy in DWT bands for a post fatigue state. Differences in coherence in post fatigue were not systematically associated with changes in DWT energy across sensory modalities, with most correlations failing to reach significance ($p > .05$).

| Post AG-ANT (GM-TA) Coherence bands | Task | Open loop | | Somatosensory | | Vestibular | | Visual | |
|---|---|---|---|---|---|---|---|---|---|
| | | r | p | r | p | r | p | r | p |
| *Low (0-3.94 Hz)* | QSEO | -0.103 | 0.75 | -0.16 | 0.618 | 0.081 | 0.803 | 0.466 | 0.127 |
| *Mid (5.92-15.78 Hz)* | QSEO | -0.141 | 0.662 | -0.354 | 0.259 | -0.078 | 0.809 | 0.541 | 0.07 |
| *High (17.75-39.45 Hz)* | QSEO | -0.199 | 0.536 | -0.505 | 0.094 | -0.406 | 0.191 | 0.567 | 0.055 |
| *Low (0-3.94 Hz)* | QSEC | -0.283 | 0.373 | -0.33 | 0.295 | -0.036 | 0.911 | 0.422 | 0.172 |
| *Mid (5.92-15.78 Hz)* | QSEC | -0.003 | 0.993 | -0.358 | 0.253 | -0.017 | 0.958 | 0.399 | 0.199 |
| *High (17.75-39.45 Hz)* | QSEC | -0.008 | 0.98 | -0.312 | 0.323 | -0.112 | 0.729 | 0.429 | 0.164 |
| *Low (0-3.94 Hz)* | FLEO | -0.32 | 0.311 | -0.366 | 0.243 | 0.123 | 0.704 | 0.319 | 0.312 |
| *Mid (5.92-15.78 Hz)* | FLEO | -0.344 | 0.273 | -0.504 | 0.095 | 0.241 | 0.451 | 0.382 | 0.22 |
| *High (17.75-39.45 Hz)* | FLEO | -0.342 | 0.277 | -0.53 | 0.076 | 0.142 | 0.66 | 0.442 | 0.15 |
| *Low (0-3.94 Hz)* | FLEC | -0.401 | 0.197 | -0.081 | 0.802 | 0.28 | 0.379 | -0.103 | 0.751 |
| *Mid (5.92-15.78 Hz)* | FLEC | -0.221 | 0.491 | -0.007 | 0.984 | 0.028 | 0.931 | 0.048 | 0.882 |
| *High (17.75-39.45 Hz)* | FLEC | -0.147 | 0.649 | -0.149 | 0.645 | -0.018 | 0.956 | 0.202 | 0.529 |

Table A7: Pearson correlation coefficients (r) and p-values between AG–ANT (SOL–TA) coherence bands and relative energy in DWT bands for a pre fatigue state. Differences in coherence in pre fatigue were not systematically associated with changes in DWT energy across sensory modalities, with most correlations failing to reach significance ($p > .05$).

| Pre AG-ANT (SOL-TA) Coherence bands | Task | Open loop | | Somatosensory | | Vestibular | | Visual | |
|---|---|---|---|---|---|---|---|---|---|
| | | r | p | r | p | r | p | r | p |
| *Low (0-3.94 Hz)* | QSEO | -0.174 | 0.609 | -0.006 | 0.985 | 0.049 | 0.886 | 0.014 | 0.967 |
| *Mid (5.92-15.78 Hz)* | QSEO | -0.125 | 0.715 | 0.118 | 0.731 | -0.032 | 0.925 | -0.004 | 0.99 |
| *High (17.75-39.45 Hz)* | QSEO | -0.173 | 0.61 | 0.093 | 0.785 | -0.021 | 0.952 | 0.01 | 0.976 |
| *Low (0-3.94 Hz)* | QSEC | -0.058 | 0.857 | -0.091 | 0.779 | -0.08 | 0.804 | 0.192 | 0.551 |
| *Mid (5.92-15.78 Hz)* | QSEC | 0.131 | 0.685 | -0.118 | 0.715 | 0.048 | 0.882 | 0.031 | 0.924 |
| *High (17.75-39.45 Hz)* | QSEC | -0.005 | 0.988 | -0.268 | 0.399 | 0.136 | 0.674 | 0.087 | 0.788 |
| *Low (0-3.94 Hz)* | FLEO | -0.373 | 0.232 | -0.205 | 0.522 | -0.219 | 0.495 | 0.372 | 0.234 |
| *Mid (5.92-15.78 Hz)* | FLEO | -0.338 | 0.283 | -0.118 | 0.716 | -0.311 | 0.325 | 0.422 | 0.172 |
| *High (17.75-39.45 Hz)* | FLEO | -0.171 | 0.596 | -0.081 | 0.802 | -0.362 | 0.248 | 0.444 | 0.149 |
| *Low (0-3.94 Hz)* | FLEC | -0.201 | 0.532 | 0.107 | 0.741 | -0.25 | 0.432 | 0.197 | 0.539 |
| *Mid (5.92-15.78 Hz)* | FLEC | -0.262 | 0.411 | 0.061 | 0.85 | -0.351 | 0.264 | 0.312 | 0.323 |
| *High (17.75-39.45 Hz)* | FLEC | -0.145 | 0.654 | -0.179 | 0.578 | -0.067 | 0.836 | 0.173 | 0.591 |

Table A8: Pearson correlation coefficients (r) and p-values between AG–ANT (SOL–TA) coherence bands and relative energy in DWT bands for post fatigue state. Differences in coherence in post fatigue were not systematically associated with changes in DWT energy across sensory modalities, with most correlations failing to reach significance ($p > .05$).

| Post AG-ANT (SOL-TA) Coherence bands | Task | Open loop | | Somatosensory | | Vestibular | | Visual | |
|---|---|---|---|---|---|---|---|---|---|
| | | r | p | r | p | r | p | r | p |
| *Low (0-3.94 Hz)* | QSEO | -0.057 | 0.861 | -0.138 | 0.668 | 0.093 | 0.774 | 0.451 | 0.141 |
| *Mid (5.92-15.78 Hz)* | QSEO | -0.141 | 0.662 | -0.353 | 0.261 | 0.026 | 0.936 | 0.551 | 0.063 |
| *High (17.75-39.45 Hz)* | QSEO | -0.301 | 0.341 | -0.42 | 0.174 | 0.061 | 0.851 | 0.51 | 0.091 |
| *Low (0-3.94 Hz)* | QSEC | -0.311 | 0.326 | -0.313 | 0.321 | -0.027 | 0.932 | 0.405 | 0.191 |
| *Mid (5.92-15.78 Hz)* | QSEC | -0.037 | 0.908 | -0.332 | 0.292 | -0.036 | 0.912 | 0.396 | 0.202 |
| *High (17.75-39.45 Hz)* | QSEC | 0.064 | 0.843 | -0.237 | 0.458 | -0.132 | 0.684 | 0.355 | 0.258 |
| *Low (0-3.94 Hz)* | FLEO | -0.398 | 0.2 | -0.345 | 0.271 | 0.034 | 0.915 | 0.363 | 0.246 |
| *Mid (5.92-15.78 Hz)* | FLEO | -0.232 | 0.469 | -0.43 | 0.163 | 0.293 | 0.355 | 0.271 | 0.393 |
| *High (17.75-39.45 Hz)* | FLEO | -0.238 | 0.457 | -0.428 | 0.166 | 0.146 | 0.651 | 0.333 | 0.291 |
| *Low (0-3.94 Hz)* | FLEC | -0.231 | 0.47 | 0.059 | 0.855 | 0.163 | 0.614 | -0.181 | 0.574 |
| *Mid (5.92-15.78 Hz)* | FLEC | -0.161 | 0.618 | 0.033 | 0.919 | -0.007 | 0.982 | 0.033 | 0.92 |
| *High (17.75-39.45 Hz)* | FLEC | -0.023 | 0.945 | -0.117 | 0.718 | -0.089 | 0.783 | 0.214 | 0.505 |